Complexation of Mn(II) by Rigid Pyclen Diacetates: Equilibrium, Kinetic, Relaxometric, Density Functional Theory, and Superoxide Dismutase Activity Studies

Zoltán Garda, Enikő Molnár, Nadège Hamon, José Luis Barriada, David Esteban-Gómez, Balázs Váradi, Viktória Nagy, Kristof Pota, Ferenc Krisztián Kálmán, Imre Tóth, et al.

Complexation of Mn(II) by Rigid Pyclen Diacetates: Equilibrium, Kinetic, Relaxometric, DFT and SOD Activity Studies.

Zoltán Garda,[†] Enikő Molnár,[†] Nadège Hamon,[‡] José Luis Barriada,[+] David Esteban-Gómez,[+] Balázs Váradi,[†,‰] Viktória Nagy,[†] Kristof Pota,[†,≠] Ferenc Krisztián Kálmán,[†] Imre Tóth,[†] Norbert Lihi,[#] Carlos Platas-Iglesias,[*,+] Éva Tóth,[§] Raphaël Tripier,[*,‡] and Gyula Tircsó[*,†]

[†] Department of Physical Chemistry, [#] Department of Inorganic and Analytical Chemistry, Faculty of Science and Technology, University of Debrecen, Egyetem tér 1, H-4032 Debrecen, Hungary

[‰] Doctoral School of Chemistry, Faculty of Science and Technology, University of Debrecen, Egyetem tér 1, H-4032 Debrecen, Hungary

[‡] Univ Brest, UMR-CNRS 6521 CEMCA, 6 avenue Victor le Gorgeu, 29238 Brest, France

[≠] Current address of the author: Department of Chemistry and Biochemistry, Texas Christian University, 2950 W. Bowie, Fort Worth, Texas 76109, United States

[+] Centro de Investigacións Científicas Avanzadas (CICA) and Departamento de Química, Universidade da Coruña, Campus da Zapateira, Rúa da Fraga 10, 15008 A Coruña, Spain.

[§] Centre de Biophysique Moléculaire, CNRS, rue Charles Sadron, 45071 Orléans, Cedex 2, France

ABSTRACT: We report the Mn(II) complexes with two pyclen-based ligands (pyclen = 3,6,9,15-tetraazabicyclo[9.3.1]pentadeca-1(15),11,13-triene) functionalized with acetate pendant arms either at positions 3,6 (**3,6-PC2A**) or 3,9 (**3,9-PC2A**) of the macrocyclic fragment. The **3,6-PC2A** ligand was synthesized in five steps from pyclen-oxalate by protecting one of the secondary amine groups of pyclen using Alloc protecting chemistry. The complex with **3,9-PC2A** is characterized by a higher thermodynamic stability ($\log K_{MnL}$ = 17.09(2) than the **3,6-PC2A** analogue ($\log K_{MnL}$ = 15.53(1), 0.15 M NaCl). Both complexes contain a water molecule coordinated to the metal ion, which results in relatively high ^{1}H relaxivities (r_{1p} = 2.72 and 2.91 $mM^{-1}s^{-1}$ for the complexes with **3,6-** and **3,9-PC2A**, respectively, 25 ºC, 0.49 T). The coordinated water molecule displays fast exchange kinetics with the bulk in both cases; the rates (k_{ex}^{298}) are 140×10^6 and 126×10^6 s^{-1} for [Mn(**3,6-PC2A**)(H_2O)] and [Mn(**3,9-PC2A**)(H_2O)], respectively. The two complexes were found to be remarkably inert with respect to their dissociation, with half-lives of 63 and 21 h, respectively, at pH 7.4 in the presence of excess Cu(II). The r_{1p} values recorded in blood serum remain constant at least over a period of 120 h. Cyclic voltammetry experiments show irreversible oxidation features shifted to higher potentials with respect to $[Mn(EDTA)(H_2O)]^{2-}$ and $[Mn(PhDTA)(H_2O)]^{2-}$, indicating that the PC2A complexes reported here have a lower tendency to stabilize Mn(III). The superoxide dismutase activity of the Mn(II) complexes was tested using the xanthine/xanthine oxidase/NBT assay at pH 7.8. The Mn(II) complexes of **3,6-PC2A** and **3,9-PC2A** are capable to assist the decomposition of superoxide anion radical. The kinetic rate constant of the complex of **3,9-PC2A** is smaller by one order of magnitude than that of **3,6-PC2A**.

INTRODUCTION

Complexes of Mn(II) containing a bound water molecule in its coordination sphere have attracted considerable attention recently, as they have been considered as potentially safe alternatives to Gd(III)-based Magnetic Resonance Imaging (MRI) contrast agents (CA).[1-3] In spite of the large efforts dedicated to the research conducted in the past 8-10 years, only a few ligand candidates represent an acceptable compromise between the seemingly contradictory requirements that need to be fulfilled for safe *in vivo* applications. The Mn(II) ion in the majority of its complexes formed with aminopolycarboxylate (APC) ligands is hexa- or heptacoordinated.[4,5] Therefore potentially penta- or hexadentate ligands can be considered for Mn(II) complexation to achieve high relaxivities owing to a water molecule bound to the metal ion (inner sphere contribution).[1] On the other hand, high thermodynamic and redox stability, as well as kinetic inertness, are required to overcome toxicity issues associated to the ad-

ministration of the Mn(II) ion in high concentration (necessary for MRI applications).[6] Mn(II) accumulation in the brain causes a neurological disorder known as manganism, expressing symptoms similar to Parkinson's disease.[7] Therefore, among the effective (i.e. high relaxivity) agents, only complexes possessing high stability and most importantly inertness can be considered as plausible candidates for CA research. However Mn(II) complexes in general are known to be labile. Among the recently studied systems there are very few inert Mn(II) complexes.[8] Within the group of open-chain ligands, the rigid CDTA[9] and its derivatives (i.e. PyC3A)[10] or PhDTA[11] complexes (Chart 1) display the best features. The acyclic $[Mn(PyC3A)(H_2O)]^-$ chelate has similar relaxation properties to that of $[Gd(DTPA)(H_2O)]^{2-}$ and it is also efficiently eliminated from rats following its intravenous injection.[12] Because of advantageous properties of the Mn(II) complexes, bifunctional ligands derived from *trans*-cyclohexane-1,2-diamine have also been prepared and characterized.[13] Moreover agents allowing for the visualization of specific organs (i.e. liver) have also been designed and characterized recently.[14] Physicochemical characterization of Gd(III) complexes have shown that the complexes of macrocyclic ligands display much better properties as far as the thermodynamics and especially the dissociation kinetics concerns.[15] The majority of macrocyclic Mn(II) complexes possess either low relaxivity (i.e. non-aquated but inert $[Mn(DOTA)]^{2-}$ or $[Mn(PCTA)]^-$ chelates)[16] or limited inertness (bisaquated Mn(II) complexes of 15-membered macrocyclic ligands such as 15Py-$aneN_5$ or 15Py-$aneN_3O_2$),[17] which limits their potential *in vivo* application. An acceptable compromise has recently been evidenced for the complexes of 1,4-DO2A and its amide derivatives (1,4-$DO2AM^{Me2}$).[18,19] These stable and inert chelates contain an average of 0.9 bound water molecule, therefore they possess only moderate relaxation enhancement. However it can substantially be enhanced (as for 1,4-$DO2AM^{Me2}$) with non-covalent binding to macromolecules such as human serum albumin (HSA).[20] The most inert Mn(II) complex was recently described by É Tóth *et al.,* which is a Mn(II) chelate formed with a 2,4-pyridyl-disubstituted bispidol ligand.[8]

Our recent studies performed with trisubstituted cyclododecane derivatives have revealed greater conditional stability for $[Mn(PCTA)]^-$ than for $[Mn(DOTA)]^{2-}$ (at pH=7.4).[16] The kinetic inertness of $[Mn(PCTA)]^-$ is sufficiently high to allow for further ligand modification, such as reduction of ligand denticity to allow the coordination of a water molecule to the metal ion. Truncating the parent PCTA ligand returns two regioisomeric ligands, the dissymmetric (3,6-disubstituted) and the symmetric (3,9-disubstituted) pyclen (pyclen = 3,6,9,15-tetraazabicyclo[9.3.1]pentadeca-1(15),11,13-triene) platforms, which can serve as alternatives to 1,4-DO2A for designing Mn(II)-based relaxation agents (Chart 1). We have recently explored some features of certain symmetric (3,9-disubstituted) PC2A derivatives. The attachment of an ethanolamine moiety, capable of protonation near to physiological pH in its Mn(II) complex, allowed us to obtain a pH-responsive Mn(II)-based smart CA (SCA) candidate (PC2A-EA).[21] Furthermore, "decorating" the **3,9-PC2A** platform with biphenyl "anchor" returns the hexadentate PC2A-BP chelator,[22] which binds HSA very efficiently, thereby allowing for the visualization of the vascular system by using low CA doses. The aim of the current study is to synthesize both disubstituted regioisomers of the PC2A ligand and characterize their complexes formed Mn(II) (thermodynamics, electrochemistry, dissociation and solvent exchange kinetics, relaxation properties and their structures), as well as the stability of complexes formed with the most abundant essential metal ions (Ca(II), Mg(II), Cu(II) and Zn(II)). The SOD activity of the regioisomeric Mn(II) complexes was also accessed with the *para*-nitro blue tetrazolium chloride (NBT) assay and compared with the data determined for Mn(SOD), $[Mn(15aneN5)(H_2O)_2]^{2+}$ and $[Mn(PCTA)]^-$.

Chart 1. Chemical structure of the ligands discussed in this work.

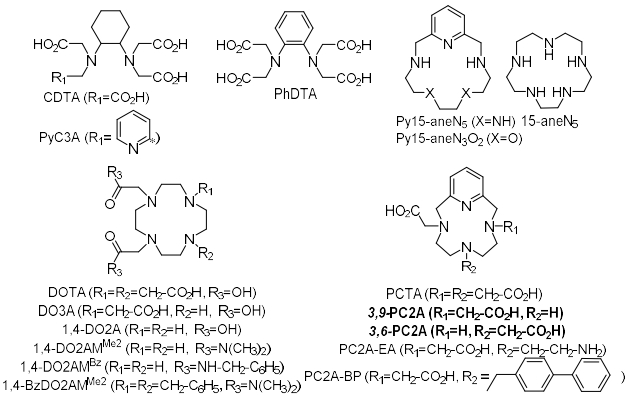

RESULTS AND DISCUSSION

Syntheses of the ligands and complexes. The symmetric **3,9-PC2A** ligand was synthesized by following published procedure reported by Kim *et al.*[23] The given synthesis relies on the addition to the pyclen macrocycle of a stoichiometric amount of the formaldehyde - sodium bisulfite addition compound, while the pH of the reaction mixture is maintained at pH = 8.55 in order to protonate (i.e. protect) the N6 nitrogen atom situated *trans* to the pyridine unit. Although this method supposed to afford the intended (3,9-disubstituted) product in quantitative yield, in our hands 3-4% of the 3,6-disubstituted product was found in the reaction mixture. These products were converted to corresponding PC2As via substitution with NaCN followed by their hydrolysis in 6 M HCl. The isomeric ligands were then separated/purified by preparative HPLC for all further studies (the details of the synthesis and analysis are included in supporting information, Fig. S1 to S8).

The synthesis of ***3,6-PC2A*** was accomplished using a procedure affording solely the 3,6-disubstituted product (Scheme 1 details of synthesis of compounds **2** – **9** and all analyses in supporting information, Scheme S1, Figures S9 to S32). The applied strategy relies on the regioselective protection of one of the secondary amines of the pyclen macrocycle, in order to introduce the two acetate arms on the remaining free secondary amines. To that aim, pyclen-oxalate **1** was first prepared as described in the literature.[24] Protection of compound **1** in the presence of 2-nitrobenzenesulfonyl chloride and $NaHCO_3$ led to compound **2** in 89% yield. Deprotection of the latter with 4 M HCl under reflux followed by a precipitation in acetone afforded compound **5**. Unfortunately, even after exchange of the counter-ion by an amberlite resin (OH^- form), the solubility of compound **5** was so low that it was not possible to perform its alkylation with two equivalents of methyl 2-bromoacetate, even under drastic conditions (DMF, reflux). We then envisioned the Fmoc protecting group as an alternative solution. Protection of compound **1** in the presence of Fmoc chloride was quantitative and deprotection of the oxalate group in acidic conditions under reflux led to compound **6**. Alkylation of the latter with two equivalents of methyl 2-bromoacetate was performed without base, but even in these conditions, partial removal of the Fmoc protecting group was observed, resulting in the formation of a mixture of the mono, di and tri-substituted pyclen derivatives. In order to avoid this side reaction, we turned our attention to the Alloc protecting group,[25] which should be resistant to the acidic conditions used for the removal of the oxalate group and to the basic conditions used for the alkylation of the acetate arms. Moreover, the conditions suggested to remove Alloc ($Pd(PPh_3)_4$ with phenylsilane as a scavenger) are compatible with the methyl esters groups used for the protection of the acetate arms.[26] Protection of pyclen oxalate **1** with one equivalent of Alloc chloride in the presence of $NaHCO_3$ led to compound **4** almost quantitatively. Removal of the oxalate group was performed under the usual acidic conditions and afforded compound **7** after exchange of the counter ion using an amberlite IRA resin (OH^- form) followed by column chromatography on neutral alumina. Alkylation of compound **7** with two equivalents of methyl 2-bromoacetate in the presence of K_2CO_3 led to the di-alkylated compound **8** in 78% yield. Removal of the Alloc group was performed with a catalytic amount of $Pd(PPh_3)_4$ and four equivalents of phenylsilane to obtain compound **9**. Finally, hydrolysis of the methyl esters under acidic conditions afforded ligand ***3,6-PC2A***, which was purified by precipitation with acetone. Complexation reactions of the ligands were done at pH = 7.2 by mixing equimolar amounts of the ligands and Mn(II) salts and the formation of the complexes were supported by ESI MS analysis and HPLC method (Supporting Information Figure S33).

Equilibrium studies. The protonation constants of the two pyclen derivatives investigated in this work have been determined by pH-potentiometry using 0.15 M as well as 1.0 M NaCl, since the determination of Cu(II) stabilities required higher ionic strengths. The protonation constants (see experimental section for details) of the ligands and their standard deviations are listed in Table 1, along with the corresponding values determined for 1,7-DO2A, 1,4-DO2A and PCTA.

The protonation sequence of PCTA and its derivatives differs from that of DOTA and other cyclen-based ligands owing to the non-symmetric nature of the pyclen macrocycle.[27] The first protonation of the PCTA occurs at the

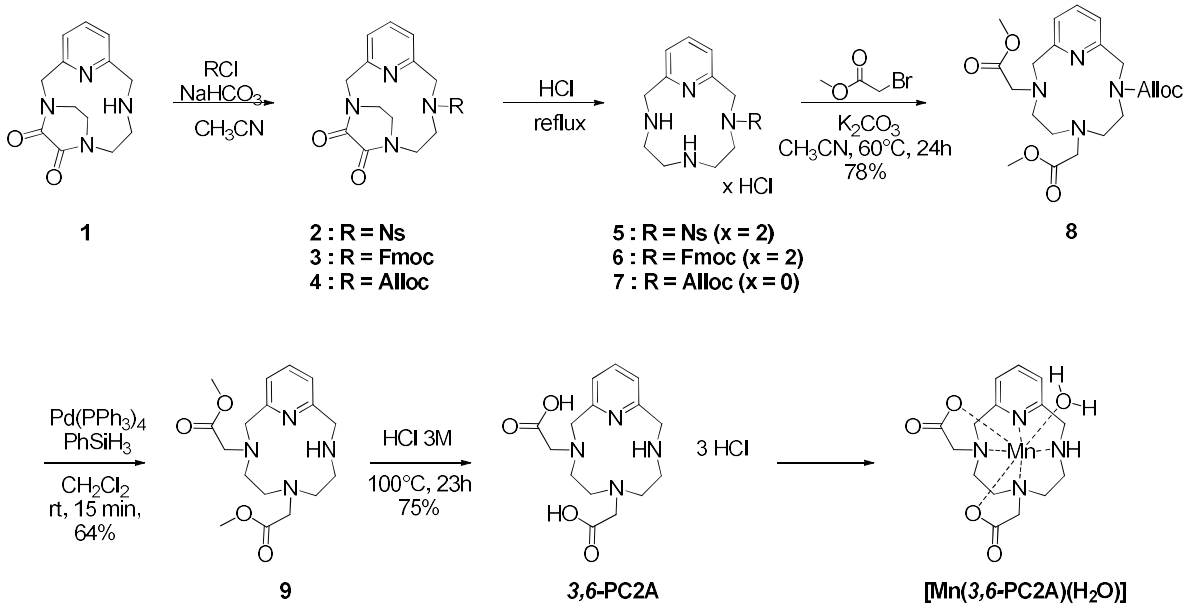

Scheme 1. Synthesis of the non-symmetric [Mn(***3,6-PC2A***)(H_2O)] complex.

Table 1. Protonation constants of the 3,9-PC2A, 3,6-PC2A, 1,7-DO2A, 1,4-DO2A PCTA and DO3A ligands T = 25°C and *I* = 0.15 M NaCl).

	3,9-PC2A	**3,6-PC2A**	*1,7*-DO2A[c]	*1,4*-DO2A[c]	PCTA	DO3A[d,f]
$\log K_1^H$	12.25(4) / 12.50[a]	10.72(1) / 10.31(1)[b]	11.69	11.44	9.97[d] / 11.36[e]	10.07
$\log K_2^H$	5.97(2) / 5.75[a]	8.37(2) / 8.59(2)[b]	9.75	9.51	6.73[d] / 7.35[e]	9.83
$\log K_3^H$	3.47(4) / 3.28[a]	3.81(2) / 3.92(3)[b]	3.97	4.14	3.22[d] / 3.83[e]	4.43
$\log K_4^H$	1.99(3) / 2.38[a]	1.26(2) / 1.56(3)[b]	2.68	1.55	1.40[d] / 2.12[e]	4.11
$\sum_{i=1}^{2} \log K_i^H$	18.22 / 18.25[a]	19.09 / 18.90	21.44	20.95	16.70[d] / 18.71[e]	19.90

[a] Data in 0.1 M KCl from Ref. 23. [b] Determined by using 1.0 M NaCl ionic background. [c] Data from Ref. 18. [d] Data from Ref. 16. [e] Data in 1.0 M KCl at 25 ºC from Ref. 29. [f] An additional protonation with $\log K_5^H$ = 1.88 was also detected.

nitrogen situated in *trans* to the pyridine nitrogen (N^6) of the pyclen macrocycle, while the second protonation occurs at the *cis*- nitrogen (N^3 or N^9), forcing the first proton to rearrange to the second *cis*- nitrogen atom to alleviate electrostatic repulsion. In agreement with this sequence, the highest protonation constant of **3,9-PC2A** ($\log K_1^H$= 12.5) can be assigned to the protonation of the N6 nitrogen atom opposite to the pyridine ring, which is in agreement with the ^{1}H-NMR titration reported by Kim et al.[23] The same authors proposed that the second protonation constant ($\log K_2^H$ = 5.75) corresponded to the pyridine nitrogen atom. However, the ^{1}H-NMR titration was performed in a relatively narrow pH range (the lowest pH at which the ^{1}H-NMR spectrum was recorded was around pH = 7). Moreover, if one assumes similar protonation sequence for the non-symmetric ligand, the second protonation constant of $\log K_2^H$ = 8.37 would be too high for the protonation of a pyridine nitrogen atom. Therefore, we feel that the protonation sequence of the PCTA proposed by S. Aime et al. holds also for the PC2A isomeric ligands. A similar protonation sequence was proposed by Drahos et al. for 6-PC1A on the basis of ^{1}H NMR experiments.[28] The $\log K_1^H$ value of **3,9-PC2A** decreases significantly upon functionalization of the secondary NH group with biphenyl (BP) or ethylamine (EA) substituents ($\log K_1^H$ = 10.45 and 11.34, respectively, *vs*. 12.25 in **3,9-PC2A**).[21,22]

The isomeric PC2A ligands were found to be less basic than the DO2A derivatives, as judged by the $\Sigma \log K_i^H$ values (Table 1). However, the parent PCTA ligand appears to be even less basic, which can be related in part to the formation of a relatively stable complex with the Na^+ ions present at high concentration in the sample (from the salt used to maintain ionic strength constant). Indeed, the protonation constants of PCTA determined in 1.0 M KCl are considerably higher than those determined in 0.15 M NaCl, [16,29] while an intermediate $\log K_1^H$ value of 10.90 was determined using *I* = 0.1 M Me_4NO_3.[30] The increasing negative charge of the ligands (i.e. increasing number of carboxylate groups capable of binding Na^+ ions) is expected to enhance the stability of the Na^+ complex, as it was also evidenced for cyclen-based chelators.[31,32] However, the protonation constants of 1,4- and 1,7-DO2A derivatives determined using 0.15 M NaCl and 0.1 M Me_4NCl electrolytes are nearly identical,[33] indicating the absence of stable Na^+ complex formation for these disubstituted derivatives. The data available in the literature for **3,9-PC2A** are also confirming our hypothesis,[23] since the values determined with the use of 0.1 M KCl and those reported here in 0.15 M NaCl do not differ considerably (the difference in the first protonation constant is only *ca*. 0.2 log units, Table 1).

The stability and protonation constants of the M(II) complexes (M = Ca, Mg, Mn, Cu and Zn) formed with **3,9-PC2A** and **3,6-PC2A** were determined by pH-potentiometric titrations (Table 2). The equilibrium model used for the fitting of the pH-potentiometric data involving the Mn(II) ion was confirmed with pH dependent ^{1}H-relaxometric titration experiments (Figure 1). A comparison of the pH-relaxivity profiles with the species distribution curves, calculated by using the stability constants obtained by pH-potentiometric titration, confirms that the equilibrium model applied for the data refinement is correct. The [Mn(**3,9-PC2A**)(H_2O)] and [Mn(**3,6-PC2A**)(H_2O)] complexes exhibit constant relaxivity (2.91 and 2.72 $mM^{-1}s^{-1}$ respectively at 0.49 T, 25 °C) in a wide pH range (4.5 - 9.5, the relaxivity of the complexes determined at 0.49 and 1.41 T at 25 °C are included in the Supporting Information Figure S34-S38). These results are characteristic of macrocyclic Mn(II) complexes with one coordinated water molecule (*q* = 1) in their inner coordination sphere (i.e. [Mn(1,4-DO2A)(H_2O)] and [Mn(6-PC1A)(H_2O)]$^+$),[4,28] and they are higher than the relaxivity of complexes with *q* = 0 (typically 1.4-1.6 $mM^{-1}s^{-1}$ as observed for [Mn($DO3A$)]$^-$ and [Mn(PCTA)]$^-$.[4,16] Lowering the pH below pH = 4.5 results in a sharp relaxivity increase, reaching r_{1p} values of 8.12 and 6.28 $mM^{-1}s^{-1}$ (at 0.49 and 1.41 T, respectively) near pH = 2.50 and 1.80 for the complexes formed with **3,6-PC2A** and **3,9-PC2A** ligands. The increase in relaxivity is associated to the protonation of the complex followed by dissociation at low pH, reaching r_{1p} values characteristic of the $[Mn(H_2O)_6]^{2+}$ complex.[34] Half of Mn(II) ions are present as the hexaaqua form at pH~2.5 in case of the 3,9-PC2A system and at pH~3.5 with

the 3,6-PC2A ligand, which suggests a significantly higher stability for the [Mn(3,9-PC2A)] complex.

The equilibrium can be described by considering only the formation of [M(L)] and monoprotonated [M(HL)] complexes for both systems (**3,9-PC2A** and **3,6-PC2A**) involving all metal ions (Table 2). The data listed in the Table 2 show that the symmetric **3,9-PC2A** forms more stable complexes with cations possessing high coordination numbers (including Mn(II)) than the non-symmetric **3,6-PC2A**, while for Cu(II) and Zn(II) the trend seems to be reversed. In fact, the stability of the Mn(II) complex formed with **3,9-PC2A** appears to be slightly higher than that of the complex formed with PCTA (log K_{MnL} = 17.09 *vs.* 16.83, respectively). This can be rationalized in terms of the increased basicity of the **3,9-PC2A** ligand upon removing one of the acetate pendant arms. However, the high basicity of the **3,9-PC2A** ligand triggers a notable decrease of the conditional stability when the basicity of the ligands is taken into account. This can be visualized by comparing the conditional equilibrium data (i.e. pMn values of the complexes) at specific conditions. When comparing the calculated pMn values (pMn = $-\log[Mn]_{free}$ of the complexes at pH = 7.4 and using 10 μM ligand and Mn(II) ion concentration) the affinity of the **3,9-PC2A** ligand towards Mn(II) is lower than that of the PCTA (pMn = 8.64 *vs.* 9.74). Nevertheless, **3,9-PC2A** appears to be a good platform for the complexation of Mn(II) as the pMn value is just slightly lower than that of the Mn(DOTA) complex calculated under identical conditions (pMn = 9.02).[16] A comparison with the data of the corresponding DO2A ligands shows the benefit of incorporating the pyridine moiety into the ligand backbone. The stability constants of the [Mn(**3,6-PC2A**)(H_2O)] and [Mn(1,4-DO2A)] complexes are nearly identical (log K_{MnL} = 15.53 and 15.68, respectively). However the calculated pMn values show one-unit difference, whereas for the [Mn(**3,9-PC2A**)(H_2O)] and [Mn(1,7-DO2A)] complexes the benefit is even more pronounced (2.5 log units in terms of stability and two orders of magnitude in terms of the conditional stability).

The complex formation for the Cu(II) systems with both **3,6-PC2A** and **3,9-PC2A** ligands is complete below pH 1.7, which is the lower limit for pH-potentiometry. Therefore, the stability constants of the Cu(II) complexes were determined by simultaneous fitting of pH-potentiometric data collected in the pH range of pH = 1.72-11.85 and UV-vis spectrophotometric titration data using batch samples with the [H^+] concentration ranging from 0.011 - 0.913 M and 0.011 - 1.020 M, respectively (Figure S39, Supporting Information). The molar absorptivities of Cu(II) and its corresponding complexes were determined independently, while those of the protonated species were fitted during the data refinement. The stability constants of the Cu(II) complexes (Table 2) are very similar to those determined previously for isomeric DO2A complexes and they are seemingly higher than the value characterizing the [Cu(PCTA)]$^-$ complex. However our recent experimental evidences suggest that the stability of the [Cu(PCTA)]$^-$ complex was underestimated in our former study.[29] The UV-Vis spectra of the protonated complex collected up to 1 M acid concentration did not indicate any measurable dissociation of the complex, as evidenced by identical spectra obtained in the acid concentration range of 0.1 – 1.0 M. One can estimate the lower limit of the stability constant of the [Cu(PCTA)]$^-$ complex as log K_{CuL} (min) = 24.

DFT calculations. In order to understand the differences in the stability of Mn(II) complexes formed with **3,9-PC2A** and **3,6-PC2A**, we turned our attention to DFT calculations. On the basis of our previous experience, we performed calculations on the [Mn(L)(H_2O)]·2H_2O systems

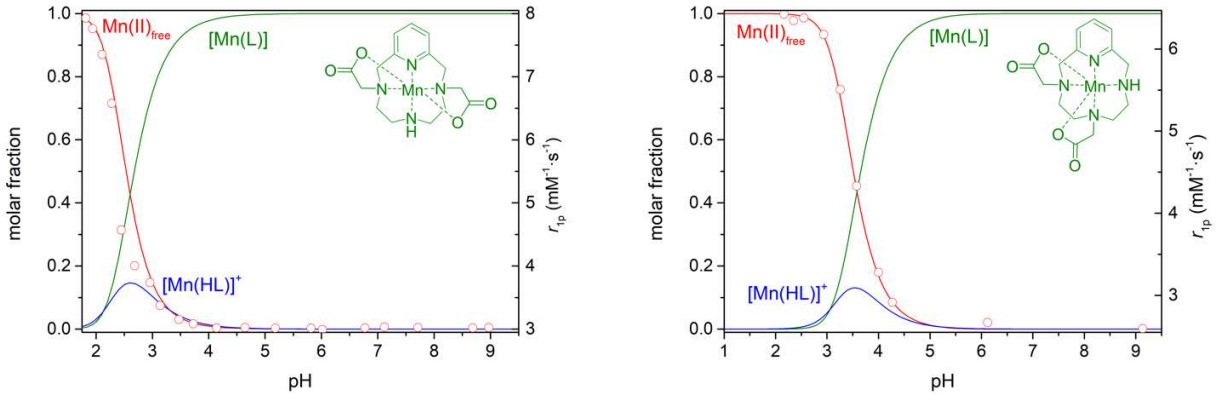

Figure 1. Species distribution diagram of the Mn(II) – L – H^+ systems ([Mn(II)]=[L]=2.04 mM, solid lines, L = **3,9-** or **3,6-PC2A**) and the normalized r_{1p} relaxivity values obtained as function of pH at 0.49 T (**3,9-PC2A**) or 1.41 (**3,6-PC2A**, red dots, T = 25 °C and *I*=0.15 M NaCl).

Table 2. Stability and protonation constants of the Mg(II), Ca(II), Mn(II), Cu(II) and Zn(II) complexes of 3,9-PC2A, 3,6-PC2A, 1,7-DO2A, 1,4-DO2A, PCTA and DO3A ligands (T = 25°C and I = 0.15 M NaCl).

	3,9-PC2A	**3,6-PC2A**	1,7-DO2A[d]	1,4-DO2A[d]	PCTA[e]	DO3A[f]
log K_{MgL}	9.84(8) / 8.40[b]	8.11(1)	–	–	12.35	11.64
log K_{MgL}^{H}	5.91(10)	5.87(9)	–	–	3.82	–
log K_{CaL}	9.92(5) / 10.0[b]	9.57(1)	8.86	8.62	12.72	12.57
log K_{CaL}^{H}	5.08(6)	5.27(9)	–	–	3.79	4.60
log K_{MnL}	17.09(2)	15.53(1)	14.64	15.68	16.83 / 16.64	16.55[g] / 19.43
log K_{MnL}^{H}	2.14(2)	3.06(4)	4.40	4.15	1.96	4.26[g] / 3.55
pMn [a]	8.64	8.09	6.52	7.27	9.74	8.66
log K_{CuL}	23.58(4)[c]	24.09(3)[c]	24.24	24.43	18.79	25.75
log K_{CuL}^{H}	2.12(8)[c]	2.37(3)[c]	3.06	2.95	3.58	3.65[j]
log K_{ZnL}	19.49(8)	20.37(1)	18.86	18.03	20.48	19.43
log K_{ZnL}^{H}	2.74(4)	2.36(1)	4.23	3.58	3.10	3.37
log K_{ZnHL}^{H}	–	–	1.78	1.65	–	–

[a] Calculated using $c_L = c_{Mn(II)} = 1 \times 10^{-5}$ M at pH = 7.4. [b] Data in 0.1 M KCl from Ref. 23. [c] I = 1.0 M NaCl; determined by simultaneous fitting of the pH-potentiometric and UV-vis data. [d] Values in 0.1 M KCl from Ref. 19 for Ca, Cu and Zn; Values in 0.15 M NaCl from Ref. 18 for Mn. [e] Values in I = 1.0 M KCl from Ref. 29, except for Mn (0.15 M NaCl, Ref. 16). [f]. Data in 0.1 M KCl from Ref. 31. [g] Data in 0.15 M NaCl from Ref. 16. [j] The formation of a diprotonated complex with log K_{MH_2L} = 1.69 (where K_{MH_2L}=[MH_2L]/[MHL][H^+]) was also reported.

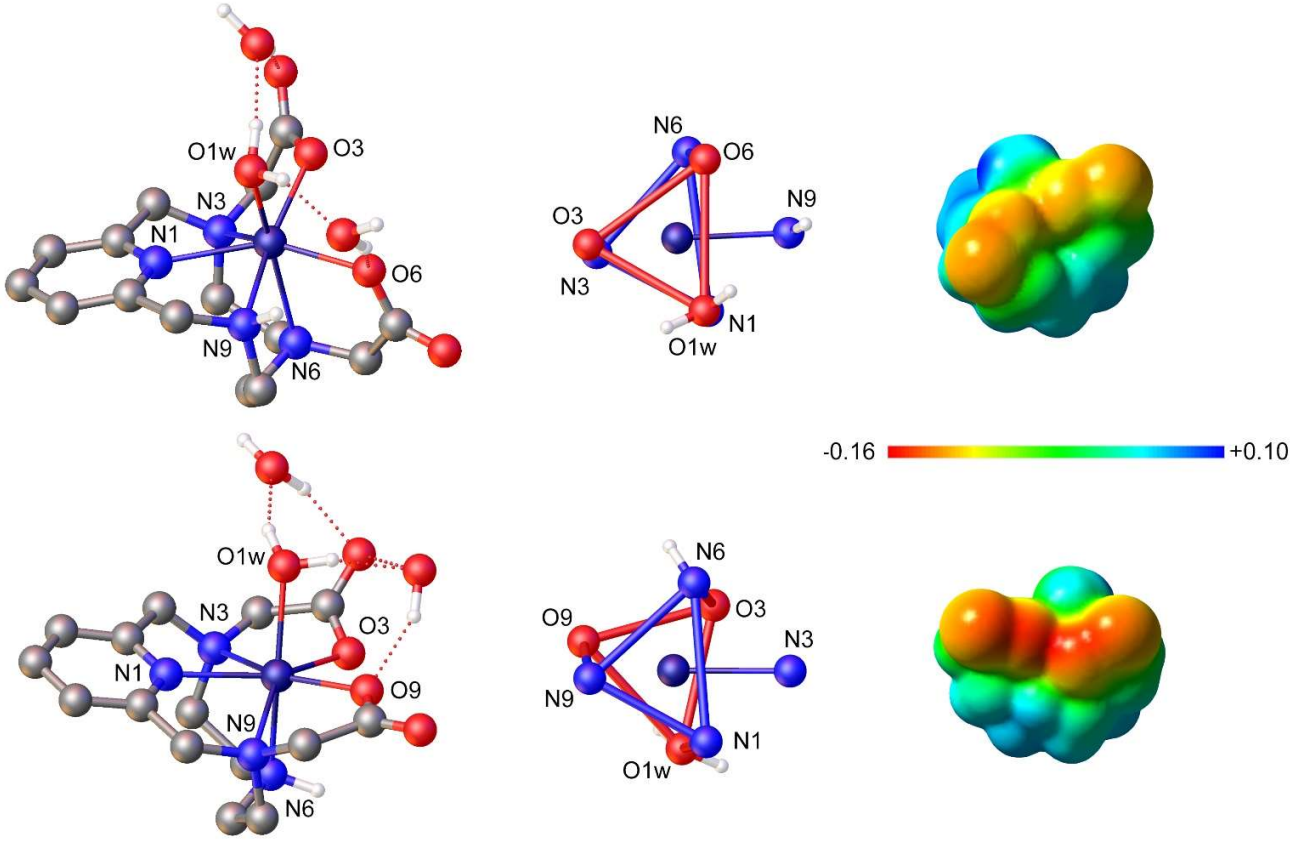

Figure 2. Geometries of the [Mn(**3,6-PC2A**)(H_2O)]·2H_2O (top) and [Mn(**3,9-PC2A**)(H_2O)]·2H_2O (bottom) systems obtained with DFT calculations at the M11/Def2-TZVPP level (left), the corresponding coordination polyhedral (center) and the electrostatic potential (a. u.) calculated on a isodensity surface defined by 0.001 of the electron density (right, views along the Mn-N1 axes).

(L = **3,6-PC2A** or **3,9-PC2A**), which include two explicit second-sphere water molecules to improve the accuracy of the calculated Mn-O_{water} distances and ^{17}O hyperfine coupling constants.[35] The optimized geometries are presented in Figure 2 (the Cartesian coordinates of the complexes are reported in the Supporting Information, Table S1 and S2), while the calculated distances of the metal coordination environments (Figure S40) are given in Table S3 (Supporting Information). Our calculations provide seven-coordinated Mn(II) for both complexes, where the coordination polyhedra can be described as a capped trigonal prisms.

The shortest bond distances of the metal coordination environment involve the O atoms of carboxylate groups, as would be expected due to the hard Lewis acid character of Mn(II). Concerning the Mn-N bonds, the strongest coordination in the **3,6-PC2A** complex is provided by the N atom of the pyridine group (Mn-N1 = 2.342 Å), as also observed in the X-ray crystal structures of Mn(II) complexes formed with pyclen derivatives [Mn(6-PC1A)Cl] (2.199 Å)[28] and [Mn(PCTA-$(OEt)_3$)]$^{2+}$(2.165 Å).[36] In these structures, the nitrogen atom of the macrocycle located *trans* to the pyridine nitrogen coordinates rather weakly to the Mn(II) ion, as evidenced by rather long Mn–N bond lengths (corresponding bond lengths are 2.349 Å and 2.431 Å in [Mn(6-PC1A)]$^+$ and [Mn(PCTA-$(OEt)_3$)]$^{2+}$ complexes, respectively. Similarly, the calculated structure of the **3,6-PC2A** complex presents a relatively long Mn-N3 distance (2.362 Å). The absence of a carboxylate pendant in *trans* to the pyridyl N atom in the complex with **3,9-PC2A** results in a dramatic shortening of the Mn-N3 bond length to 2.289 Å, while the distance to the pyridyl N atom is also shortened significantly to 2.314 Å. Based on these bond lengths, it appears that the presence of a carboxylate group in *trans* to the pyridyl N atom hinders the coordination of the amine N atom at position 6. The absence of a pendant arm at this position, such as in the complex with **3,9-PC2A**, likely releases steric strain, allowing for a more tight coordination of the N atoms at positions 1 and 6 (N1 and N3 in Figure 2).

Dissociation of the Mn(II) complexes. Metal chelates used in medical diagnosis and therapy must be kinetically inert so they do not dissociate to release free metal ion and ligand during the time they remain *in vivo*. Although Mn(II) is an essential metal ion, prolonged exposure to Mn(II) causes clinical signs and symptoms resembling, but not identical, to Parkinson's disease. Thus, the kinetics of decomplexation is a critical issue that must be considered to develop Mn(II)-based CA candidates. Therefore, the dissociation kinetics of the [Mn(**3,6-PC2A**)(H_2O)] and [Mn(**3,9-PC2A**)(H_2O)] complexes were studied by various methods to evaluate their inertness.

Metal exchange reactions occurring with Zn(II) at pH = 6.0. First, we evaluated the rate of the metal exchange reaction occurring with Zn(II) under the conditions proposed by Caravan and coworkers (metal exchange reaction initiated by 25 equiv. of Zn(II) at pH = 6.0, set by 50 mM MES buffer), using T_2 relaxometry at 37 °C.[10] Because Zn(II) forms more stable complexes than Mn(II), it can be used to trigger the dissociation. Owing to the high r_{2p} relaxivity of the Mn(II) ion released as a result of dissociation (64.3 and 54.2 $mM^{-1}s^{-1}$ at 1.41 T and 25 and 37 °C, respectively), measuring relaxation rates as function of time is a very sensitive method to probe the inertness of Mn(II)

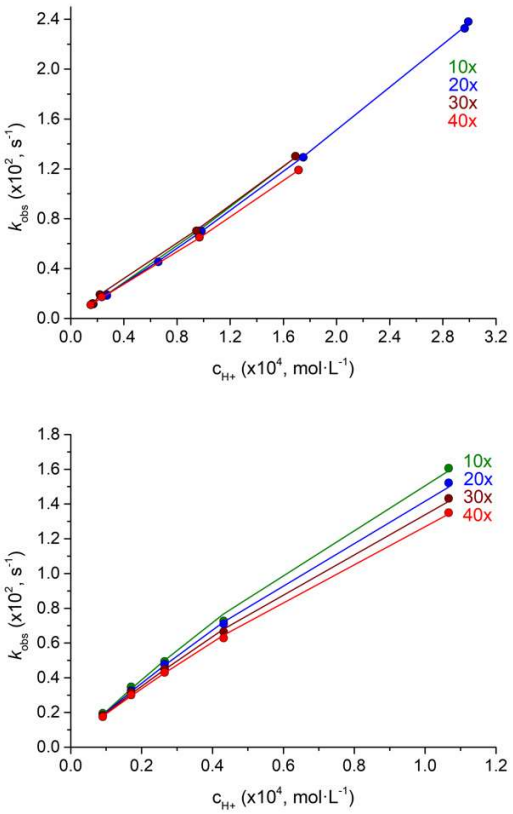

Figure 3. Dissociation rates (k_{obs}) of the Mn(II) complexes formed with **3,6-** (top) and **3,9-PC2A** (bottom) obtained in the presence of excess Cu(II) (10, 20, 30 and 40 equiv.) and plotted as a function of H^+ ion concentration (I = 0.15 M NaCl, T = 25 °C).

complexes. The pseudo-first-order rate constants determined for the dissociation of [Mn(**3,6-PC2A**)(H_2O)] and [Mn(**3,9-PC2A**)(H_2O)] complexes are (3.28±0.03)×10^{-4} and (5.43±0.04)×10^{-4} s^{-1}, respectively (Figures S41, Supporting Information). These values are similar than that reported previously for [Mn(PyC3A)(H_2O)] (6.76±0.04) ×10^{-4} s^{-1}),[10] which was proposed as an alternative to Gd(III)-based CAs. These data indicate that the isomeric ligand form Mn(II) complexes endowed with different inertness, with the [Mn(**3,6-PC2A**)(H_2O)] complex dissociating more slowly. However, the differences are less pronounced than those observed recently for the Gd(III) complexes formed with pyclen mono and dipicolinates.[37]

Metal exchange reactions occurring with Cu(II). We have performed a detailed dissociation kinetics study by evalu-

ating the rate constants of metal exchange reactions occurring with the Cu(II) ion in the pH-range of 3.55-4.75 (**3,6-PC2A**) and 3.97-5.02 (**3,9-PC2A**). As it can be seen in Figure 3, the k_{obs} rate constants increase with increasing H^+ ion concentration, showing a saturation-like behavior for the [Mn(**3,9-PC2A**)(H_2O)] complex, and a second order dependence on H^+ ion concentration for [Mn(**3,6-PC2A**)(H_2O)]. However, the k_{obs} values decrease with increasing Cu(II) ion concentration for both complexes (the effect of the metal ion is more pronounced for [Mn(**3,9-PC2A**)(H_2O)]). These data indicate that the Mn(II) complexes dissociate spontaneously and following the acid assisted pathway. However, in the presence of large excess of Cu(II) the formation of the heterodinuclear [Mn(L)Cu] complex decelerates the reactions, presumably by reducing the concentration of kinetically more reactive protonated form(s) of the complexes. Taking into account the possible reaction pathways, the rate of dissociation of the Mn(II) complexes can be expressed as in Eqn (1):

$$-\frac{d[\mathrm{Mn(L)}]}{dt} = k_{obs}[\mathrm{Mn(L)}]_t = k_0[\mathrm{Mn(L)}] + k_{\mathrm{H}}[\mathrm{Mn(HL)}] + k_{\mathrm{H}}^{\mathrm{H}}[\mathrm{Mn(H_2L)}] + k_{\mathrm{Cu}}[\mathrm{Mn(L)Cu}] \qquad (1)$$

where k_{obs} is a pseudo-first-order rate constant, $[Mn(L)]_t$ is the total concentration of the Mn(II) chelates, k_o is the rate constant characterizing the spontaneous dissociation, k_H and k_H^H are the rate constants corresponding to the acid-assisted dissociation, and k_M is the rate constant characterizing the metal-assisted dissociation pathway. Taking into account the concentration of various complexes (Mn(L), protonated Mn(HL) or Mn(H_2L) and dinuclear (Mn(L)Cu) those existence was evidenced by a stopped-flow method Figure S42), as well as the protonation ($K_{Mn(HL)}$ and $K_{Mn(H_2L)}$) and stability constants ($K_{Mn(L)Cu}$) of the corresponding intermediates, the following rate equation can be derived (k_1=k_H×$K_{Mn(HL)}$, k_2=k_H^H×$K_{Mn(HL)}$×$K_{Mn(HL)}$ and k_3=k_{Cu}×$K_{Mn(L)Cu}$):

$$k_{obs} = \frac{k_0 + k_1[\mathrm{H^+}] + k_2[\mathrm{H^+}]^2 + k_3[\mathrm{Cu^{2+}}]}{1 + K_{\mathrm{Mn(HL)}}[\mathrm{H^+}] + K_{\mathrm{Mn(HL)}}K_{\mathrm{Mn(H_2L)}}[\mathrm{H^+}]^2 + K_{\mathrm{Mn(L)Cu}}[\mathrm{Cu^{2+}}]} \qquad (2)$$

Eqn (2) takes into account all the rational dissociation pathways expected to occur under the experimental conditions used in the current study. Based on the first attempts of data fitting, Eqn (2) was further simplified, as the rate constant characterizing the spontaneous (k_o) dissociation of the complexes was found to be either negative ([Mn(**3,6-PC2A**)(H_2O)]) or a value with a large standard deviation. This is likely because under these experimental conditions dissociation occurs mainly via an acid assisted pathway, while the contribution of the spontaneous dissociation to the overall reaction is negligible. In case of the Mn(II) complex of the 3,6-isomer we could not obtain reliable data for the second protonation constant of the complex ($K_{Mn(H_2L)}$), whereas the $K_{Mn(HL)}$ value determined from kinetic data was found to be 25 times higher (3.6×10^3 M^{-1}) for the Mn(II) complex of 3,9-isomer than the one determined by pH-potentiometric titration (1.38×10^2 M^{-1}).

The rate constants obtained by fitting the pseudo-first-order (k_{obs}) rate data are presented and compared with those determined for Mn(II) chelates of PCTA, PC2A-BP, PC2A-EA, 6-PC1A, DOTA, DO3A, 1,4-DO2A and 1,7-DO2A in Table 3. The comparison of the k_1 rate constants indicates that removal of an acetate pendant arm from the PCTA ligand results in a considerable drop in the inertness of their Mn(II) complexes. A similar drop in terms of inertness is observed when comparing the rate constants characterizing the acid-assisted dissociation of [Mn(DOTA)] and [Mn(DO3A)], and even a more significant decrease on going from [Mn(DO3A)] to the regioisomeric [Mn(1,7-DO2A)] and [Mn(1,4-DO2A)(H_2O)] complexes.

Table 3. Rate and equilibrium constants and half-lives of dissociation (pH = 7.4) for the Mn(II) complexes formed with 3,6- and 3,9-PC2A compared with those determined for PCTA, PC2A-BP, PC2A-EA, 6-PC1A, DOTA, DO3A, 1,4-DO2A and 1,7-DO2A (T = 25°C and I = 0.15 M NaCl).

	k_o (s^{-1})	k_1 ($M^{-1}s^{-1}$)	k_2 ($M^{-2}s^{-1}$)	k_3 ($M^{-1}s^{-1}$)	$K_{Mn(HL)}$	$K_{M(L)M}$	$t_{1/2}$ (h)
PCTA[a]	$(7.0\pm0.1)\times10^{-2}$ [b]	1.09×10^{-1} [b] / 8.2×10^{-2}	3.5×10^2	1.8×10^{-6}	91 [c]	38 (Zn)	5.90×10^4
3,9-PC2A	–[d]	221±5	–	$(3.6\pm0.7)\times10^{-2}$	$(3.6\pm0.5)\times10^3$	26±3	21.0
3,6-PC2A	–[d]	70±1	$(1.5\pm0.4)\times10^5$	$(2.6\pm0.7)\times10^{-2}$	1.15×10^3 [c]	16±2	63.2
PC2A-BP[e]	–[d]	16.9	–	–	1350	–	286
PC2A-EA[f]	–[d]	0.6	–	–	102	–	8.00×10^3
6-PC1A[g]	–[d]	2020	8×10^7	–	8.92×10^4 [c]	–	2.40
DOTA[a]	1.8×10^{-7}	0.04	1.6×10^3	1.5×10^{-5}	4.57×10^5 [c]	68 (Zn)	1037
DO3A[a]	–[d]	0.45	3.2×10^2	–	1.82×10^4 [c]	–	1.1×10^4
1,4-DO2A[h]	–[d]	100	1.6×10^6	–	1.41×10^4 [c]	–	48
1,7-DO2A[h]	–[d]	85	3.0×10^6	–	2.51×10^4 [c]	–	58

[a] Data from Ref. 16. [b] Determined by stopped-flow technique in highly acidic solutions, Ref. 16. [c] The value obtained by pH-potentiometric titration was fixed during the calculations. [d] Fixed to 0 for the data fitting. [e] Data from Ref. 22. [f] Data from Ref. 21. [g] Data from Ref. 28. [h] Data from Ref. 18. [I] Half-lives of dissociation were calculated at pH = 7.4 by using the rate constants and 0.01 mM M(II) ion concentration.

The dissociation of regioisomeric [Mn(1,7-DO2A)] or [Mn(1,4-DO2A)(H_2O)] complexes occurs with very similar rates (in the studied pH-range), while isomeric [Mn(PC2A)(H_2O)] complexes behave differently as far as their dissociation kinetics is concerned. The most striking difference can be seen when comparing the rates of acid assisted dissociation (k_1), which is slightly more than 3 times higher for the [Mn(**3,9-PC2A**)(H_2O)] complex than-for [Mn(**3,6-PC2A**)(H_2O)]. These differences are also reflected in the half-life values ($t_{1/2}$) of dissociation calculated at pH = 7.4 in the presence of 0.01 mM exchanging metal ion (Table 3). Furthermore, the protonation constant of the [Mn(**3,9-PC2A**)(H_2O)] complex estimated form the kinetic data appeared to be nearly three times higher than that of [Mn(**3,6-PC2A**)(H_2O)], which indicates that the [Mn(**3,9-PC2A**)(H_2O)] complex is more prone to the protonation (i.e. formation of protonated intermediate) than [Mn(**3,6-PC2A**)(H_2O)]. The electrostatic potential calculated with DFT on the molecular surface defined by 0.001 a.u isosurface of the electron density (Figure 2),[38] provides a straightforward explanation for this effect. The two complexes present rather different charge distributions (Figure 2). As expected, the most negative electrostatic potential resides on the negatively charged carboxylate groups. The electrostatic potential on the molecular surface of [Mn(**3,9-PC2A**)(H_2O)] reaches more negative values (ca. -0.16 a.u.) than for [Mn(**3,6-PC2A**)(H_2O)] (ca. -0.10 a.u., Figure 2). As a result, the complex with **3,9-PC2A** is more readily protonated, favoring the proton-assisted dissociation mechanism.

Dissociation of the Mn(II) complexes in human blood serum. Proteins present in the blood serum (albumin is the most abundant serum protein) are known to bind the essential metal ions relatively strongly. MRI CAs are administered in the order of grams per injection, and thus plasma proteins could potentially initiate transmetallation processes. This issue is particularly critical for Mn(II) complexes whose thermodynamic stability is lower than the stability of the chelates formed with essential metal ions such as Zn(II), Cu(II). The binding of Mn(II) to HSA results in an increase of relaxivity from 7.92 $mM^{-1}s^{-1}$ measured for the Mn(II) ion in water solution to 97.2 $mM^{-1}s^{-1}$ at 0.47 T, 25 °C for the Mn(HSA) adduct.[39] Therefore, mixing a kinetically labile and thermodynamically less stable chelate with a Seronorm® solution is expected to provoke the dissociation of the chelate, resulting in a notable increase in the relaxation rate of the sample, as observed for Mn(II) chelates formed with open-chain ligands.[9] However, the relaxation rate of the samples containing [Mn(**3,6-PC2A**)(H_2O)] and [Mn(**3,9-PC2A**)(H_2O)] chelates remain constant for at least 120 and 190 h respectively, indicating the negligible dissociation of the complex in serum solution prepared from Seronorm (Figure S43, Supporting Information). One should note that the relaxivity of the complexes measured in Seronorm solutions is somewhat higher (r_{1p} are 2.98 and 3.26, while r_{2p} are 4.95 and 6.34 $mM^{-1}s^{-1}$, respectively at 1.41 T and 25 °C, Supporting Information, Figure S38) also than that measured in pure aqueous solution indicating a weak interaction of the uncharged complexes with serum components.

^{17}O NMR measurements. The efficiency of Mn(II) based MRI contrast agents depends on different microscopic parameters, an important one being the exchange rate of the coordinated water molecule(s), k_{ex}.[40] Water exchange can be conveniently determined from the temperature dependence of ^{17}O transverse relaxation rates, which are largely dominated by the scalar mechanism.[41] The observed reduced transverse relaxation rates $1/T_{2r}$ depend on the water exchange rate at 298 K, k_{ex}^{298}, and its activation enthalpy $\Delta H^{\ddagger}$, the relaxation time of the electron spin T_{2e}^{298}, and the ^{17}O hyperfine coupling constant $A/\hbar$. Furthermore, ^{17}O NMR chemical shifts provide direct access to $A/\hbar$.[42]

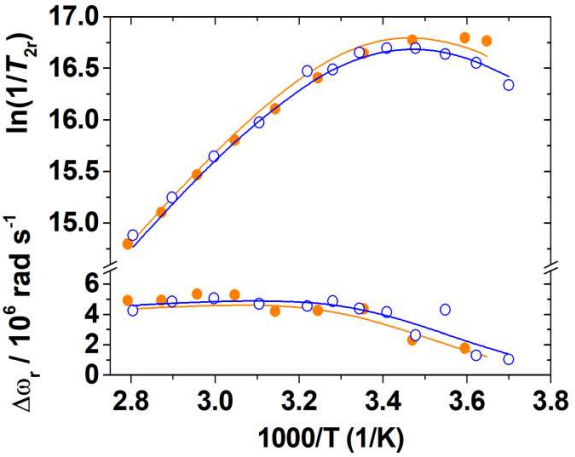

Figure 4. Reduced transverse ^{17}O relaxation rates and chemical shifts for the Mn(II) complexes of **3,6-PC2A** (open blue circles) and **3,9-PC2A** (closed orange circles) measured at 9.4 T. The solid lines correspond to the fits of the data as described in the text.

The reduced transverse relaxation rates and chemical shifts recorded for [Mn(**3,6-PC2A**)(H_2O)] and [Mn(**3,9-PC2A**)(H_2O)] are very similar (Figure 4), both indicating a changeover from a fast-exchange regime at high temperatures to an intermediate exchange regime at low temperatures. The two complexes present a maximum in the plot of $1/T_{2r}$ at about the same temperature, which anticipates very similar water exchange rates. The relaxivity at this maximum can be used to estimate the hydration number of the complexes using the method proposed by Gale.[43] We obtained a value of q of 0.7, which confirms the formation of monohydrated complexes in solution.

The fits of the reduced relaxation rates and chemical shifts afforded the parameters shown in Table 4. According to the parameters obtained in this analysis, the contribution of the electron spin relaxation term $1/T_{1e}$ to

Table 4. Best-fit parameters obtained from the analysis of ^{17}O NMR chemical shifts and reduced relaxation rates of [Mn(*3,6*-PC2A)(H_2O)], [Mn(3,9-PC2A)(H_2O)] and [Mn(1,4-DO2A)(H_2O)] recorded at 9.4 T.[a]

	3,6-PC2A	*3,9*-PC2A	*1,4*-DO2A
k_{ex}^{298} / 10^6 s^{-1}	140 ± 25	126 ± 12	1134
$\Delta H^{\ddagger}$ / kJ mol^{-1}	38.2 ± 3.9	37.5 ± 2.4	29.4
$A_O/\hbar$. / 10^6 rad s^{-1}	-44.6 ± 1.8	-42.4 ± 1.9	-43.0
$1/T_{2e}^{298}$ / 10^8 s^{-1}	1.8 ± 0.6	1.1 ± 0.3	1.0

[a] Data from Ref.4.

the transverse relaxation rate varies between 79-10 % and 49-8 % for [Mn(**3,6-PC2A**)(H_2O)] and [Mn(**3,9-PC2A**)(H_2O)], respectively, in the temperature range 0-75 °C. The relatively small contribution of the electron spin relaxation in the fast exchange limit ensures that the value calculated for the water exchange rate is correct.

In the case of Mn(II), water exchange is typically accelerated upon complexation. The water exchange rates determined for the two complexes are very similar, and indeed, they are about five times higher than that on the aqua ion (k_{ex}^{298} = 28.2 × 10^6 s^{-1}). However, the water exchange rates determined for [Mn(**3,6-PC2A**)(H_2O)] and [Mn(**3,9-PC2A**)(H_2O)] are still ~3.5 times lower than that reported for [Mn(EDTA)(H_2O)]$^{2-}$ (k_{ex}^{298} = 471 × 10^6 s^{-1}).[4] The structurally related [Mn(1,4-DO2A)(H_2O)] complex presents a water exchange rate that is one order of magnitude higher (Table 4). This fast water exchange was ascribed to an important degree of steric compression around the water binding site, which favors water exchange following a dissociative mechanism. This steric compression is even higher in [Mn(1,7-DO2A)], which does not contain a coordinated water molecule. Thus, the incorporation of a pyridyl group into the 12-membered macrocyclic unit favors the coordination of a water molecule to the metal center (Table S3, Supporting Information).

The water exchange rates determined for [Mn(**3,6-PC2A**)(H_2O)] and [Mn(**3,9-PC2A**)(H_2O)] can be regarded as rather low when compared to those reported for typical Mn(II) chelates. The similar water exchange rates measured for the two complexes are in line with the structures obtained with DFT calculations, which predict very similar Mn-O_{water} distances (2.270 and 2.279 Å for [Mn(**3,6-PC2A**)(H_2O)] and [Mn(**3,9-PC2A**)(H_2O)], respectively, Table S3, Supporting Information). DFT calculations provided ^{17}O $A_O/\hbar$. values of -39.8 × 10^6 and -40.7 × 10^6 rad·s^{-1}, which are in excellent agreement with those obtained from the fits of the ^{17}O NMR data. These values fall in the upper range of the values normally observed for Mn(II) complexes (-31 × 10^6 to -46 × 10^6 rad·s^{-1}).[4,43] The excellent agreement between the experimental and calculated data confirms that the assumption that q = 1 is correct. Thus, the slightly higher relaxivity observed for the **3,9-PC2A** complex is likely related to a slightly shorter Mn···H distance, as the dipolar relaxation rate of the coordinated water molecule is inversely proportional to the sixth power of this distance.

CV measurements. The potential oxidation of a Mn(II) based contrast agent may have a negative impact in the relaxivity of the agent, as Mn(III) complexes with polyaminopolycarboxylate ligands generally present lower relaxivities with respect to the Mn(II) counterparts.[44] Thus, we carried out cyclic voltammetry experiments using aqueous solutions of the complexes in 0.15 M NaCl (Figure 5). The cyclic voltammogram of the complex with **3,6-PC2A** recorded at a scan rate of 50 mV s^{-1} displays an oxidation peak at E_{ox} = +862 mV and a reduction peak at E_{red} = +579 mV ($\Delta E_{1/2}$ = 720 mV *vs*. Ag/AgCl). The cyclic voltammogram of the **3,9-PC2A** complex is characteristic of an irreversible system, showing an oxidation peak at E_{ox} = +838 mV and a very faint reduction signal at E_{red} ~ +340 mV. Electrochemically irreversible Mn(II)/Mn(III) redox processes are quite common. This has been attributed to the lack of ligand field stabilization for the high spin d5 configuration of Mn(II), with consequent large inner sphere contribution to electron transfer.[45] The electrochemical redox behavior of the complexes appears to be controlled by diffusion, as the cathodic and anodic current intensities vary linearly with the square root of the scan rate in the range 10–300 mV s^{-1} for **3,6-PC2A** and **3,9-PC2A** respectively (Figures S44-S45, Supporting Information).

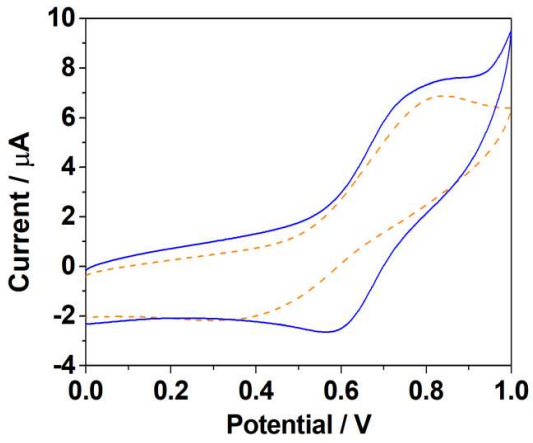

Figure 5: Cyclic voltammograms recorded for the Mn^{2+} complexes of **3,6-PC2A** (blue solid line) and **3,9-PC2A** (dashed orange line). Conditions: 2 mM, pH = 7.1, 0.15 M NaCl, scan rate 50 mV/s, potentials reported *vs*. Ag/AgCl).

The Mn(II) complexes with **3,6-PC2A** and **3,9-PC2A** present very similar E_{ox} values, and therefore similar abilities to stabilize Mn(III). The E_{ox} values determined for the

complexes of **3,6** and **3,9-PC2A** complexes are shifted to higher potentials with respect to the values reported for $[Mn(EDTA)(H_2O)]^{2-}$ (E_{ox} = 769 mV) and $[Mn(PhDTA)(H2O)]^{2-}$ (E_{ox} = 813 mV) under the same conditions,[11] which indicates that the PC2A complexes reported here have a lower tendency to stabilize Mn(III). The complexes reported here are also more resistant to oxidation than the 1,4-$DO2A^{2-}$and 1,7-$DO2A^{2-}$ analogues, which are characterized by half-wave potentials of 636 and 705 mV (*vs.* Ag/AgCl).[18]

SOD activity of [Mn(3,6-PC2A)(H_2O)] and [Mn(3,9-PC2A)(H_2O)] complexes. The SOD activity of the Mn(II) complexes was tested using the xanthine/xanthine oxidase/NBT assay at pH 7.8.[46] The inhibition curves as a function of complex concentration are shown in Figure S46 (Supporting Information). It is important to note that Mn(II) salts exhibit significant SOD activities,[47] therefore the species distributions were recalculated for each Mn(II) concentration used in the SOD activity studies. These distribution curves clearly confirm that the Mn(II) is bound to the ligands under the conditions of SOD activity studies and the complexes do not dissociate even at the μM concentration level. Thus, the free Mn(II) does not affect the decomposition of superoxide anion radical.

The IC_{50} value was estimated to be 26.1 μM and 136 μM for [Mn(**3,6-PC2A**)(H_2O)] and [Mn(**3,9-PC2A**)(H_2O)], respectively. However, the Mn(II) complex of PCTA did not exhibit any SOD activity up to a 240 μM concentration level. From the IC_{50} values, it is also possible to calculate the kinetic rate constant, k_{McCF}, for the SOD activity using Eqn (3):

$$k_{McCF} = k_{NBT} \times \frac{[NBT]}{IC_{50}} \qquad (3)$$

where k_{NBT} is 5.94×10^4 $M^{-1}s^{-1}$ for NBT (at pH 7.8; In our assay, the concentration of NBT was 45 μM). Since k_{McCF} does not depend on the concentration of the detector molecule and its nature, it is frequently used to compare directly the activities of different complexes. The calculated k_{McCF} values are summarized in Table S4 (Supporting Information). The results demonstrate that Mn(II) complexes of **3,6-PC2A** and **3,9-PC2A** are capable to assist the decomposition of the superoxide anion radical. The kinetic rate constant of the complex of **3,9-PC2A** is smaller by one order of magnitude than that of **3,6-PC2A**, while the PCTA analogue does not have any activity. The estimated IC50 values are relatively high, therefore the McCord-Fridovich assay cannot represent catalytic conditions, so both catalytic and stoichiometric reaction can be envisioned. To explore the reaction between the Mn(II) complexes and the superoxide anion in detail, dedicated stopped-flow experiments were carried out. Thus, the dismutation of the superoxide anion was monitored at 260 nm using catalytic conditions ($c(O_2^{\bullet-})/c(complex) \sim 40$). The characteristic kinetic traces are shown in the supporting information (Figure S47). The presence of manganese complexes slightly accelerates the disproportionation of the superoxide anion; however, the decomposition is slow, yet faster than the non-catalysed pathway. The decomposition is noticeably faster for the Mn(II) complex of **3,6-PC2A** than that for **3,9-PC2A**, an observation that is in good agreement with those obtained for the McCord-Fridovich assay. Since catalytic conditions were applied to study the decomposition, it is reasonable to assume that the investigated complexes act as a real yet weak catalyst for superoxide dismutation.

The presence of inner sphere water molecule likely contributes to the degradation of the superoxide anion radical. The coordinated water molecule in the PC2A complexes provides an accessible coordination sites for interaction with $O_2^{\bullet-}$ or peroxides. The $[Mn(PCTA)]^-$ complex does not possess any metal bound water molecule, preventing the redox processes between the superoxide anion and Mn(II). The less negative electrostatic potential on the molecular surface of the [Mn(**3,6-PC2A**)(H2O)] complex likely facilitates a stronger coordination of the superoxide radical, resulting in an enhanced catalytic activity compared with the **3,9-PC2A** analogue (Figure 2). Nevertheless, it is important to note that the catalytic activities of these complexes are considerably smaller than those reported for other Mn(II) complexes bearing a N-tripodal scaffold or pentadentate ligands derived from ethylenediamine.[48,49]

CONCLUSIONS

In conclusion, in the current study we have shown that the Mn(II) complexes formed with **3,6-** and **3,9-PC2A** regioisomeric ligands possess different physico-chemical

Table 5 Comparison of the most relevant physico-chemical data of the Mn(II) complexes formed with 3,6-PC2A and 3,9-PC2A ligands (25 °C and 0.15 M NaCl).

	[Mn(**3,6-PC2A**)(H_2O)]	[Mn(**3,9-PC2A**)(H_2O)]
log $K_{[Mn(L)]}$	15.53	17.09
pMn[a]	8.03	8.64
$t_{1/2}$ (h)[b]	63.2	21.0
k_{ex}^{298} ($\times 10^6$ s^{-1})	140	126
E_{ox} / mV [c]	862	838
r_{1p}/r_{2p}^{298} ($mM^{-1}s^{-1}$) [d]	2.72/3.49	2.91/3.96
r_{1p}/r_{2p}^{298} ($mM^{-1}s^{-1}$) [e]	2.98/4.95	3.26/6.34

[a] pMn values were calculated at pH = 7.4 by using 0.01 mM Mn(II) and ligand concentration, as suggested by É. Tóth and co-workers[28]; [b] the half-lives (h) of dissociation were calculated at pH = 7.4 by using the rate constants and 0.01 mM Cu(II) ion concentration. [c] Scan rate 50 mV s-1, pH 7.1, 0.15 M NaCl. [d] At 0.49 T field strength. [e] In Seronorm at 1.41 T field strength and 25 °C.

properties. The relevant physico-chemical data (thermodynamic and redox stability, dissociation and solvent exchange kinetics, and relaxivity values (at 25 °C)) are collected and compared in Table 5. The most pronounced differences among the two regioisomeric complexes concern the stability, dissociation kinetics and relaxivity values. The [Mn(**3,9-PC2A**)(H_2O)] complex possesses better thermodynamic stability (higher log $K_{[Mn(L)]}$ and pMn) and relaxometric properties (r_{1p}/r_{2p} at 25 and 37 °C at both field strengths assessed), while the [Mn(**3,6-PC2A**)(H_2O)] chelate has superior kinetic inertness, based on metal exchange reactions occurring with essential metal ions. In overall, both chelates can serve as suitable "building blocks" when tailoring inert Mn(II) complexes for safe MRI applications, as well as for designing "smart"/responsive imaging probes.

EXPERIMENTAL SECTION

Materials and methods. Reagents were purchased from ACROS Organics and from Aldrich Chemical Co and used without further purification. Dialysis membranes (cut-off 100-500 Da) were purchased from Repligen. All solvents were dried and distilled prior to use according to standard methods. Compound **1**[24] was synthesized as previously described. The **3,9-PC2A** ligand was prepared according to literature procedures, starting form commercially available dipicolinic acid and diethylenetriamine (details of the synthesis are included in the Supproting Information).[23,50] The corresponding Mn(II) complex was prepared by mixing stock solutions of the ligand and metal ion and pH adjustment to the desired value. Syntheses of compounds **2**, **3**, **5**, **6**, the Mn(II) complex of **3,6-PC2A** and corresponding analyses including HPLC, NMR and HRMS are given in the supporting information (Scheme S1, Figure S1 to S29). Analytical HPLC was performed on a Prominence Shimadzu HPLC/LCMS-2020 equipped with a UV SPD-20 A detector. HPLC separation on Prep C18 AQ 5 µM 250× 4.6 mm column was performed with H2O+ 0.1% TFA and MeOH as eluents at a flow rate of 1 mL/min and UV detection at 254 and 350 nm. NMR spectra were recorded at the "Services communs" of the University of Brest. ^{1}H and ^{13}C NMR spectra were recorded using Bruker Avance 500 (500 MHz), Bruker Avance 400 (400 MHz), or BrukerAMX-3 300 (300 MHz) spectrometers. HRMS analyses were performed on a HRMS Q-Tof MaXis instrument equipped with ESI, APCI, APPI and nano-ESI sources (at the Institute of Organic and Analytic Chemistry (ICOA), University of Orléans, Orléans, France). Numbering of the hydrogens and carbons of the molecules are given in the supporting information.

Synthesis. Compound 4. A solution of compound **1** (3.10 g, 11.9 mmol) and $NaHCO_3$ (2.00 g, 23.8 mmol, 2 equiv) in CH_3CN (238 mL) was stirred at room temperature for 40 min. Alloc-Cl (1.33 mL, 12.5 mmol, 1.05 equiv) was added dropwise to this solution. The reaction mixture was stirred at room temperature for 14h. Salts were filtered and the filtrate was evaporated to dryness. The residue was taken up in dichloromethane and the residual salts were filtered. The filtrate was evaporated to dryness to give **4** (4.08 g, 11.8 mmol, 99%, mixture of two rotamers) as a white foam. ^{1}H NMR (500 MHz, $CDCl_3$) δ 7.52 (t, J = 7.7 Hz, 1H, H13 of the first rotamer), 7.51 (t, J = 7.7 Hz, 1H, H13 of the second rotamer), 7.10 (d, J = 7.5 Hz, 1H, H12 of the first rotamer), 7.01 (d, J = 8.0 Hz, 1H, H14 of the first rotamer), 7.0 (d, J = 8.0 Hz, 1H, H14 of the second rotamer), 6.96 (d, J = 7.5 Hz, 1H, H12 of the second rotamer), 5.81 (ddt, J = 16.3, 10.5, 5.8 Hz, 1H, H20 of the first rotamer), 5.62 (ddd, J = 16.1, 10.8, 5.5 Hz, 1H, H20 of the second rotamer), 5.53 (d, J = 16.9 Hz, 2H, H2a of both rotamers), 5.19 (dd, J = 17.2, 1.3 Hz, 1H, H21a of the first rotamer), 5.13 (dd, J = 10.4, 1.0 Hz, 1H, H21b of the first rotamer), 4.99 (dd, J = 10.5, 1.2 Hz, 1H, H21b of the second rotamer), 4.92 (dd, J = 17.2, 1.5 Hz, 1H, H21a of the second rotamer), 4.61 (d, J = 14.3 Hz, 1H, CH_2 pyclen), 4.55 (d, J = 14.8 Hz, 1H, CH_2 pyclen), 4.47 (d, J = 5.8 Hz, 2H, H19 of one rotamer), 4.42-4.31 (m, 2H), 4.21 (d, J = 13.8 Hz, 1H), 4.14 (m, 1H), 4.06 (d, J = 16.9 Hz, 1H, H4 of the first rotamer), 4.04 (d, J = 16.9 Hz, 1H, H4 of the second rotamer), 3.88 – 3.78 (m, 4H), 3.75 – 3.51 (m, 7H), 3.31 (ddd, J = 14.7, 11.2, 3.9 Hz, 1H, CH_2 pyclen), 3.13 – 3.00 (m, 4H). ^{13}C NMR (125 MHz, $CDCl_3$) δ 162.9, 162.8 (C16), 159.3, 159.2 (C17), 156.5, 156.4, 156.18 (C11, C18), 153.3, 153.0 (C1), 137.3, 137.1 (C13), 132.2 (C20), 122.1, 121.61 (C12), 119.8, 119.7 (C14), 118.2, 117.2 (C21), 66.1, 65.7 (C18), 58.7, 57.5, 57.0, 56.8, 51.1, 49.9, 48.9, 48.8, 47.8, 46.8, 45.5, 45.4 (CH_2 pyclen). ESI-HR-MS (positive) m/z calcd. for $[C_{17}H_{21}N_4O_4]^+$: 345.1557, found: 345.1557, $[M+H]^+$; calcd. for $[C_{17}H_{20}N_4NaO_4]^+$: 367.1377, found: 367.1374, $[M+Na]^+$.

Compound 7. A solution of compound **4** (4.04 g, 11.7 mmol) in 2M HCl (50 mL) was stirred at 100°C for 5.5 h and then cooled down to room temperature before addition of H_2O (70 mL) and amberlist A21 resin (75.0 g) to remove the excess of the acid. The mixture was slowly stirred for 1 h before filtration of the resin which was washed with water and MeOH. The filtrate was evaporated to dryness to give a yellow oil. Exchange of the counter-ion was performed on a column of amberlite IRA 458 (OH^- form, 56 mL) with MeOH as an eluent. Purification of the oil was performed by several precipitations (first precipitation with MeOH/Et_2O, 2nd precipitation with hot CH_3CN, third precipitation with MeOH/AcOEt) and by column chromatography on neutral alumina (eluent: CH_2Cl_2/MeOH 100/0 to 100/2) to give compound **7** (3.37 g, 11.5 mmol, 98%, 1/1 mixture of two rotamers) as a white solid. ^{1}H NMR (500 MHz, D_2O) δ 7.67 (t, J = 7.3 Hz, 2H, H13 of the two rotamers), 7.19 (d, J = 6.5 Hz, H12 of the first rotamer), 7.18 (d, J = 6.5 Hz, H12 of the second rotamer), 7.12 (d, J = 7.6 Hz, 2H, H14 of the two rotamers), 6.00 (ddt, J = 16.3, 10.8, 5.6 Hz, 1H, H17 of the first rotamer), 5.71 (ddt, J = 16.0, 10.3, 4.9 Hz, 1H, H17 of the second rotamer), 5.36 (d, J = 17.2 Hz, 2H, H18a of the first rotamer), 5.28 (d, J = 10.6 Hz, 2H, H18b of the first rotamer), 5.06 (d, J = 10.0 Hz, 1H, H18b of the second rotamer), 5.04

(d, J = 16.7 Hz, 1H, H18a of the second rotamer), 4.65 – 4.55 (m, 6H, H16 of the first rotamer), 4.45 (d, J = 4.6 Hz, 2H, H16 of the second rotamer), 3.91 (d, J = 7.9 Hz, 4H), 3.76 – 3.66 (m, 4H), 2.82 (s, 4H), 2.61 – 2.55 (m, 2H), 2.45 (d, J = 3.2 Hz, 4H), 2.37 (s, 2H). ^{13}C NMR (126 MHz, D_2O) δ 161.9 (Cq), 161.8 (Cq), 160.9 (C15 of the first rotamer), 160.7 (C15 of the second rotamer), 159.1 (Cq), 158.7 (Cq), 140.7 (C13), 135.4 (C17 of the first rotamer), 135.2 (C17 of the second rotamer), 123.4, 122.7, 122.7 (C12 and C14 of both rotamers), 121.1 (C18 of the first rotamer), 119.5 (C18 of the second rotamer), 69.4 (C16 of the first rotamer), 69.1 (C18 of the second rotamer), 55.2 (CH_2), 54.7 (CH_2), 53.9 (CH_2), 50.5 (CH_2), 49.7 (CH_2), 49.6 (CH_2), 48.8 (CH_2), 48.8 (CH_2), 48.7 (CH_2), 48.6 (CH_2). ESI-HR-MS (positive) m/z calcd. for $[C_{15}H_{23}N_4O_2]^+$: 291.18155, found: 291.1817, $[M+H]^+$; 251 and 207 = fragmentations.

Compound 8. A solution of compound **7** (0.50 g, 1.73 mmol) and K_2CO_3 (0.72g, 5.18 mmol, 3 equiv) in CH_3CN (91 mL) was stirred at 60°C 30 min. A solution of methyl 2-bromoacetate (0.335 mL, 3.54 mmol, 2.05 equiv) in CH_3CN (91 mL) was added to this solution dropwise. The reaction mixture was stirred at 60°C for 20 h, cooled down to room temperature and salts were filtered off. The filtrate was evaporated to dryness and the residue was taken up in dichloromethane. Residual salts were filtered and the filtrate was evaporated to dryness. The residue was dissolved in the minimum of CH_2Cl_2 and hexane was added in large excess. After 4 h, an oil appeared on the wall of the flask. Isolation of the supernatant and evaporation to dryness gave compound **8** (590 mg, 1.36 mmol, 78%, mixture of two rotamers) as a pale yellow oil. ^{1}H NMR (500 MHz, $CDCl_3$) δ 7.58 (m, 1H, H13), 7.25 – 7.18 (m, 1H), 7.10 (d, J = 6.5 Hz, 1H), 5.92 – 5.76 (m, 1H, H21), 5.20 (m, 1H, H22a), 5.12 (d, J = 5.8 Hz, H22b), 4.56 (m, 2H, CH_2 pyclen), 4.50 (m, 2H, H20), 4.03 (d, J = 4.5 Hz, 2H, CH_2 pyclen), 3.72 – 3.52 (m, 11H, 2*OCH_3 + CH_2 pyclen), 3.40 (br s, 1H, CH_2 acetate), 3.26 (br s, 1H, CH_2 acetate), 2.69 (m, 4H, CH_2 pyclen), 2.61 (br s, 1H, CH_2 pyclen), 2.48 (br s, 1H, CH_2 pyclen). ^{13}C NMR (125 MHz, $CDCl_3$): Some C presents two signals because of the presence of rotamers, δ 171.6, 171.5 (C=O), 157.9, 157.7, 156.6, 156.4 (C1 and C11), 155.8, 155.5 (C19), 137.6, 137.4 (C13), 132.8, 132.7 (C21), 122.7, 122.4, 122.2, 121.6 (C12 and C14), 117.2, 117.1 (C22), 65.9, 65.9 (C20), 59.6, 59.5, 55.9, 55.7, 54.5, 54.1 (CH_2 pyclen and C16, C16'), 51.3, 51.2 (C18, C18'), 50.9, 50.4, 50.3, 50.2, 48.9, 48.3, 46.6, 46.0 (CH_2 pyclen). ESI-HR-MS (positive) m/z calcd. for $[C_{21}H_{31}N_4O_6]^+$: 435.2238, found: 435.2234, $[M+H]^+$; calcd. for $[C_{21}H_{30}N_4NaO_6]^+$: 457.2058, found: 457.2055, $[M+Na]^+$; 351, 363 = fragmentations.

Compound 9. A solution of compound **8** (0.31 g, 0.71 mmol) in CH_2Cl_2 (71 mL) at 0°C was bubbled with N_2 for 45 min and then warmed to room temperature before addition of $Pd(PPh_3)_4$ (0.082 g, 0.07 mmol, 0.1 equiv) and phenylsilane (0.352 µL, 2.85 mmol, 4 equiv). The reaction mixture was stirred at room temperature for 15 min, concentrated to V = 2mL and immediately purified by column chromatography on alumina gel (eluent: CH_2Cl_2/MeOH/Et_3N 100/0/1 to 100/1/1) to give compound **9** (0.16 g, 0.46 mmol, 64%) as a brown oil. ^{1}H NMR (500 MHz, $CDCl_3$) δ 7.50 (t, J = 7.6 Hz, 1H, H13), 7.01 (d, J = 7.6 Hz, 1H, H12), 6.96 (d, J = 7.6 Hz, 1H, H14), 4.02 (s, 2H, H10), 3.90 (s, 2H, H2), 3.57 (s, 3H, OCH_3), 3.55 (s, 3H, OCH_3), 3.45 (s, 2H, H16), 3.31 (s, 2H, H16'), 2.95 (t, J = 6.1 Hz, 2H, H4), 2.75 – 2.67 (m, 2H, H7), 2.63 (m, 2H, H8), 2.28 (t, J = 6.1 Hz, 2H, H5). ^{13}C NMR (75 MHz, $CDCl_3$) δ 172.1, 171.7 (C=O), 158.6, 158.4 (C1, C11), 136.8 (C13), 121.5, 121.4 (C14 and C12), 61.2 (C2), 58.2 (C16), 55.5 (C16'), 54.6 (C4), 53.8 (C7), 52.6 (C10), 51.5 (OCH_3), 51.3 (OCH_3), 49.1 (C5), 44.4 (C8). ESI-HR-MS (positive) m/z calcd. for $[C_{17}H_{27}N_4O_4]^+$: 351.2027, found: 351.2026, $[M+H]^+$; calcd. for $[C_{17}H_{26}N_4NaO_4]^+$: 373.1846, found: 373.1843, $[M+Na]^+$; calcd. for $[C_{17}H_{28}N_4O_4]^{2+}$: 176.1049, found: 176.1047, $[M+2H]^{2+}$.

3,6-PC2A. A solution of compound **9** (0.133 g, 0.38 mmol) in 3M HCl (5.4 mL) was stirred at 100°C for 23 h and then cooled down to room temperature before addition of acetone in large excess. The white precipitate was filtered on cotton and washed several times with acetone, then dissolved in water. Evaporation of water gave compound **3,6-PC2A** (0.123 g, 0.28 mmol, 75%) as a yellow oil. ^{1}H NMR (500 MHz, D_2O) δ 7.89 (t, J = 7.8 Hz, 1H, H13), 7.41 (d, J = 7.8 Hz, 1H, H12), 7.37 (d, J = 7.8 Hz, 1H, H14), 4.79 (peak hidden under D_2O, 2H, H2), 4.60 (m, 2H, H10), 4.36 (s, 2H, H16), 3.54 (s, 2H, H16'), 3.50 (t, J = 5.2 Hz, 2H, H4), 3.21 (br s, 2H, H8), 2.94 (br s, 2H, H5), 2.77 (br s, 2H, H7). ^{13}C NMR (125 MHz, D_2O) δ 177.9, 171.1 (C=O), 152.2 (C11), 151.6 (C1), 142.8 (C13), 125.6 (C12), 124.8 (C14), 62.5 (C2), 58.5 (C16), 57.9 (C4 and C16'), 54.6 (C7), 53.0 (C10), 52.5 (C5), 48.5 (C8). ESI-HR-MS (positive) m/z calcd. for $[C_{15}H_{23}N_4O_4]^+$: 323.1714, found: 323.1714, $[M+H]^+$; calcd. for $[C_{15}H_{24}N_4O_4]^{2+}$: 162.0893, found: 162.0889, $[M+2H]^{2+}$.

Thermodynamic Stability Studies. Metal stock solutions were prepared from the highest analytical grade chemicals, and their concentrations were determined by complexometric titration with standardized Na_2H_2EDTA and eriochrome black T indicator in the presence of ascorbic acid and potassium hydrogen tartrate for $MnCl_2$, murexide indicator for $CaCl_2$ and $CuCl_2$, eriochrome black T for $MgCl_2$ and xylenol orange in the presence of hexamethylenetetramine for the solution of $ZnCl_2$. The concentration of the ligand stock solution was determined by pH-potentiometric titrations. For determining the protonation constants of the ligand, pH potentiometric titrations were carried out with 0.15 M NaOH, using 0.002 M ligand solutions. The ionic strength was set to 0.15 M by using NaCl. The titrated samples (starting volume of 6 mL) were stirred mechanically and thermostated at 25 °C by a circulating water bath (±0.1 °C). The protonation constants of the ligand (log K_i^H) are defined as follows:

$$K_i^H = \frac{[H_iL]}{[H_{i-1}L][H^+]} \qquad (4)$$

where i = 1, 2, ..., 4 and $[H_{i-1}L]$ and $[H^+]$ are the equilibrium concentrations of the ligand (i = 1), its protonated forms (i = 2, ..., 4) and hydrogen ion, respectively. The

stability constants are defined as follows (where i = 0 for the ternary hydroxide complex and i = 1 or 2 for the protonated complexes):

$$K_{\mathrm{ML}} = \frac{[\mathrm{ML}]}{[\mathrm{M}][\mathrm{L}]} \text{ and } K_{\mathrm{MH_iL}} = \frac{[\mathrm{MH_iL}]}{[\mathrm{MH_{i-1}L}][\mathrm{H^+}]} \quad (5)$$

To avoid the effect of CO_2, N_2 gas was bubbled through the solutions during the titrations process. The pH-potentiometric titrations were performed with a Metrohm 785 DMP Titrino titration workstation with the use of a Metrohm 6.0234.100 combined electrode in the pH range of 1.75-11.8. For the calibration of the pH meter, KH-phtalate (pH = 4.005) and borax (pH = 9.177) buffers were used, and the H^+ concentrations were calculated from the measured pH values by applying the method proposed by Irving *et al*.[51] A solution of approximately 0.01 M HCl was titrated with a 0.15 M NaOH solution (0.15 or 1.00 M NaCl), and the differences between the measured and calculated pH values (for the points with pH < 2.4) were used to calculate the $[H^+]$ from the pH values measured in the titration experiments. The measured points with pH > 11.0 of the acid-base titration were used to calculate the ionic product of water which was found to be 13.847 (0.15 M NaCl) and 13.826 (1.0 M NaCl) under our experimental conditions. For the calculation of the equilibrium constants, the PSEQUAD program was used.[52] The stability constants of the metal complexes (except for Cu(II)) were determined using the direct pH-potentiometric method by titrating samples with 1:1 metal-to-ligand ratios (the number of fitted data pairs were between 150-200), allowing 1 min for the sample equilibration to occur. The stability constants of the Cu(II) complexes was too high to be determined by pH-potentiometry, hence a direct UV-vis spectrophotometric method was used. The spectrophotometric measurements were performed with a JASCO V-770 UV-vis-NIR spectrophotometer at 25 °C, using semi-micro 1.0 cm cells. For the determination of the stability constants the absorbance was measured at 8 different acid concentrations (falling in the acid concentration range of 0.11 – 1.00 M) at 17 wavelengths between 640 and 800 nm (the concentration of the complex was 3.0 mM). A pH-potentiometric titration of the Cu(II) complexes was also performed in the pH range 1.75-11.85 with a starting volume of 6 mL, $c_{Cu(II)} = c_{PC2As} = 2.0$ mM and these data were treated simultaneously with those obtained the UV-vis-NIR spectrophotometric measurements.

Kinetic Studies. The inertness of the [Mn(**3,6-PC2A**)(H_2O)] and [Mn(**3,9-PC2A**)(H_2O)] complexes were studied by various methods. The transmetallation reaction initiated by with Zn(II) ions was monitored by measuring the T_2 relaxation times as a function of time at pH = 6.0, set by 50 mM 2-(*N*-morpholino)ethanesulfonic acid (MES) buffer in the presence of 25 equivalents of Zn(II) ions at 37 °C. These conditions were used recently by P. Caravan *et al*. and employed here to obtain to have data that can be directly compared to [Mn(PyC3A)(H_2O)] we have adopted the same method.[10]

Metal exchange reactions occurring between the complex and Cu(II) (in the presence of 10-40-fold excess to ensure pseudo-first-order conditions) was investigated at 25 °C and 0.15 M NaCl ionic strength by using JASCO V-770 UV-vis-NIR spectrophotometer at 290 nm. The concentration of the complexes were set to 0.294 and 0.398 mM for the Mn(II) complexes of **3,6-** and **3,9-PC2A**, respectively, while the concentration of $CuCl_2$ was as follows: 3.06, 6.12, 9.18 and 12.20 mM for [Mn(**3,6-PC2A**)(H_2O)] and 3.98, 7.96, 11.94 and 15.92 mM for [Mn(**3,9-PC2A**)(H_2O)]. All the kinetic studies were performed by using a noncoordinating buffer, *N,N'*-dimethyl piperazine (DMP, $\log K_2^H = 4.19$) at 0.05 M concentration to maintain constant pH in the samples in the pH range of 3.55-4.75 and 3.98-5.02). The values of the pseudo-first-order rate constants (k_{obs}) were determined using the following equation: $A_t=(A_r-A_p)e^{-kobs\times t}+A_v$, where A_t is the absorbance at time t, A_r is the absorbance of the reactants, A_p is the absorbance of the products.

Serum stability of the Mn(II) complexes was studied by following the r_{1p} relaxivities of the complexes over time using 1.0 mM solutions in Seronorm™ (Seronorm = commercially available lyophilized human blood serum, Sero, Stasjonsveien, Norway) at pH = 7.39 and 25 °C.

Relaxation properties. The ^{1}H longitudinal (T_1) and transverse (T_2) relaxation times were measured by using Bruker Minispec MQ-20 and MQ-60 NMR Analyzers. The temperature of the sample holder was set 25.0 (±0.2) °C and controlled with a circulating water bath thermostat. The r_{1p} values for the investigated complexes were determined by means of inversion recovery method (180° – τ – 90°), averaging 4-6 data points obtained at 12 different τ delay times, while r_{2p} data were collected by using Carl-Purcell-Meiboom-Gill (CPMG) spin-echo pulse sequence. Relaxivities were determined by published procedures in samples of 0.3-0.4 mL volume. pH were either set by using a 0.05 M 4-(2-hydroxyethyl)-1-piperazine-ethanesulfonic acid (HEPES) buffer (pH = 7.4) or monitored (pH-profiles) using a Metrohm 827 pH lab pH-meter and a Metrohm 6.0234.100 combined electrode in the pH range of 1.75-11.8.

^{17}O NMR measurements. Variable-temperature ^{17}O NMR measurements of aqueous solutions of the complexes (c_{MnL} = 4.02 mmol/kg, pH 6.86, and c_{MnL} = 3.99 mmol/kg, pH 8.83, respectively) were performed on a Bruker Avance III 400 MHz spectrometer (9.4 T, 54.2 MHz) in the temperature range 0–85 °C. The temperature was calculated after calibration with ethylene glycol and MeOH.[53] Acidified water ($HClO_4$, pH = 3.3) was used as diamagnetic reference. Previous studies showed that an acidified water reference or the corresponding Zn^{2+} complex at identical concentration and pH as the paramagnetic Mn(II) sample gave identical results.[Hiba! A könyvjelző nem létezik.] The ^{17}O transverse (T_2) relaxations times were obtained by the Carl-Purcell-Meiboom-Gill spin-echo technique.[54] To eliminate the susceptibility contributions to the chemical shift the sample was placed in a glass

sphere fixed in a 10 mm NMR tube.[55] To improve sensitivity, the amount of ^{17}O was enriched by adding $H_2{}^{17}O$ (10 % $H_2{}^{17}O$, CortecNet) to achieve approximately 1 % ^{17}O content in the samples.

The ^{17}O NMR data were analyzed according to the Swift Connick equations.[56] The least-squares fit of the data were performed using Visualizeur/Optimiseur[57] running on a MATLAB 8.3.0 (R2014a) platform.

Cyclic voltammetry. Cyclic voltammetry experiments were carried out using a 797 VA Computrace potentiostat/galvanostat from Metrohm (Herisau, Switzerland) equipped with a typical three electrode cell. A glassy carbon rotating disk electrode (stirring rate of 2000 rpm) was employed as the working electrode, while the counter electrode was a platinum rod. Potentials were recorded using a Ag/AgCl reference electrode filled with 3 mol L^{-1} KCl. Aqueous solutions of the complexes in 0.15 M NaCl were purged with high purity (99.999 %) nitrogen over 30 seconds before recording the cyclic voltammograms. Sweep rates from 5 and up to 500 mV s^{-1} were used. The starting and end potentials were set to 0.0 V, while the first vertex potential was +1.0 V.

DFT calculations. Density functional theory calculations were performed with the Gaussian 16 program package (version B.01).[58] Geometry optimizations of the [Mn(**3,6-PC2A**)(H_2O)]·$2H_2O$, and [Mn(**3,9-PC2A**)(H_2O)]·$2H_2O$ systems were carried out with the M11 functional,[59] which belongs to the family of hybrid-meta GGA functionals (Supporting Information Tables S1-S3). The def2-TZVPP basis set was used throughout.[60] Bulk solvent effects (water) were included with the integral equation formalism implementation of the polarizable continuum model (IEFPCM).[61] Frequency calculations were conducted to confirm the nature of the optimized geometries as true energy minima.

SOD activity measurements. Xanthine, xanthine oxidase (0.5 U/mg) and nitro blue tetrazolium chloride (NBT) were purchased from Sigma-Aldrich. In order to study the SOD activity of the Mn(II) complexes of **3,6-**, **3,9-PC2A** and PCTA, the xanthine/xanthine oxidase system was used to generate the superoxide anion radical ($O_2^{\bullet-}$). The radical reacts with para-nitro blue tetrazolium chloride (NBT) to produce diformazan with a characteristic molar absorptivity at 560 nm. The formation of diformazan can readily be followed by UV-vis spectroscopy. The addition of the Mn(II) complexes to this system prevents the reduction of NBT. The assay was carried out in phosphate buffer (0.05 M) containing NBT (45 μM) and xanthine (200 μM). The reaction was initiated by adding an appropriate amount of xanthine oxidase to produce around 0.020-0.028 min^{-1} rate of the absorbance change at 560 nm. First, the reaction was monitored in a blank sample (without the addition of any Mn(II) complex) for 3-4 min. Then the Mn(II) complex was added to the same sample and the absorbance was monitored for further 4 min. The corresponding rates were obtained by fitting the experimental data to a straight line.

The inhibition of xanthine oxidase by the complexes was tested via the conversion of xanthine to urate and the reactions were followed by UV-vis spectroscopy at 290 nm. The rate of urate production was the same in the presence and absence of the complexes, thus the xanthine oxidase is not inhibited by the complexes.

The SOD activity was expressed as the IC_{50} value, which was converted into rate constants as described elsewhere in detail (Supporting information Table S_4).[62]

Stopped-flow measurements. The decomposition of superoxide anion (O_2^-) was studied with fast kinetic experiments using an Applied Photophysics SX-20 stopped-flow instrument equipped with a photomultiplier tube as the detector. The kinetic traces were recorded at 25 °C using 2 mm optical path length cells. The measurements were carried out in a water:DMSO 1:1 solvent mixture and the stopped-flow experiments were carried out in sequential mode to circumvent the relatively slow homogenization of the solvents. The first syringe was filled with water, the second with KO_2 in DMSO, while the third contained the Mn(II) complex dissolved in 1:1 DMSO and aqueous HEPES buffer (50 mM, pH 7.75). In the first part of the experiments, the aging loop was filled with the 1:1 mixture of the first and second solution to produce a KO_2 reagent (in water:DMSO 1:1 solvent mixture). After 40 s incubation time, the mixture was reacted with the solution of the third syringe and the progress of the reaction was monitored at 260 nm. This incubation time is necessary to avoid spectral disturbances. The O_2^- solutions were freshly prepared before each experiment by dissolving solid KO_2 (Acros Organics) in vigorously stirred DMSO containing 18-crown-6 (Sigma-Aldrich). The formation of and ion pair between O_2^- and K^+ incorporated in the crown ether improves the solubility of KO_2. This carrier molecule does not affect the kinetic experiments. The concentration of the superoxide stock solution was determined by the stopped-flow method using the same protocol described above. In the absent of catalyst, the initial absorbance values were used to determine the concentration using the molar absorbance of the superoxide anion at 260 nm, $\varepsilon(O_2^-) = 2686\ M^{-1}cm^{-1}$.

ASSOCIATED CONTENT

Supporting Information

The supporting Information is available free of charge at http://pubs.acs.org/doi/xxx/xxxx.

Synthesis of ***3,9*-PC2A**, **2**, **3**, **5**, **6** and [Mn(**3,6-PC2A**)(H_2O)], NMR and HRMS, HPLC traces, UV-Vis titrations, voltammograms, DFT data and the results of SOD activity studies (PDF).

AUTHOR INFORMATION

Corresponding Authors

*E-mail: carlos.platas.iglesias@udc.es (C. P.-I.)

*E-mail: raphael.tripier@univ-brest.fr (R. T.)
*E-mail: gyula.tircso@science.unideb.hu (Gy. T.)

Author Contributions

The manuscript was written through contributions of all authors. All authors have given approval to the final version of the manuscript.

ACKNOWLEDGMENT

G. T., F. K. K., I. T. and N. L. are grateful for the financial support of the Hungarian National Research, Development and Innovation Office (NKFIH K-120224, 128201, 134694 and PD-128326 projects) for their financial support. Gy. T. and C. P.-I. gratefully acknowledge the COST Action CA15209 "European Network on NMR Relaxometry" and the bilateral Hungarian-Spanish science and technology cooperation program (2019-2.1.11-TÉT-2019-00084). This publication and the scientific research were supported by the Gedeon Richter's Talentum Foundation established by Gedeon Richter Plc. (Gedeon Richter PhD fellowship). R.T. acknowledges the Ministère de l'Enseignement Supérieur et de la Recherche, the Centre National de la Recherche Scientifique and the "Service Commun" of NMR facilities of the University of Brest. Gy.T. acknowledges the University of Brest for his invited Professor position in 2014. D. E.-G. and C. P.-I. thank Ministerio de Economía y Competitividad (CTQ2016-76756-P) and Xunta de Galicia (ED431B 2020/52) for generous financial support. The authors are indebted to Centro de Supercomputación de Galicia (CESGA) for providing the computer facilities. . E.T. acknowledges financial support from the French National Research Agency (grant ANR-18-CE18-0008).

REFERENCES

(1) (a) Gupta, A.; Caravan, P.; Price, W. S.; Platas-Iglesias, C.; Gale, E. M. Applications for Transition-Metal Chemistry in Contrast-Enhanced Magnetic Resonance Imaging. *Inorg. Chem.* **2020**, *59*, 6648–6678; (b) Botta, M.; Carniato, F.; Esteban-Gómez, D.; Platas-Iglesias, C.; Tei, L. Mn(II) compounds as an alternative to Gd-based MRI probes. *Future Med. Chem.* **2019**, *11*, 1461–1483.

(2) (a) Drahos, B.; Lukes, I.; Tóth, E. Manganese(II) Complexes as Potential Contrast Agents for MRI. *Eur. J. Inorg. Chem.* **2012**, 2012, 1975–1986. (b) Pan, D.; Schmieder, A. H.; Wickline, S. A.; Lanza, G. M. Manganese-Based MRI Contrast Agents: Past, Present, and Future. *Tetrahedron* **2011**, *67*, 8431–8444.

(3) Wahsner, J.; Gale, E. M.; Rodríguez-Rodríguez, A.; Caravan, P. Chemistry of MRI Contrast Agents: Current Challenges and New Frontiers. *Chem. Rev.* **2019**, *119*, 957–1057.

(4) Rolla, G. A.; Platas-Iglesias, C.; Botta, M.; Tei, L.; Helm, L. ^{1}H and ^{17}O NMR Relaxometric and Computational Study on Macrocyclic Mn(II) Complexes. *Inorg. Chem.* **2013**, *52*, 3268–3279.

(5) (a) Pujales-Paradela, R.; Carniato, F.; Uzal-Varela, R.; Brandariz, I.; Iglesias, E.; Platas-Iglesias, C.; Botta, M.; Esteban-Gómez, D. A pentadentate member of the picolinate family for Mn(II) complexation and an amphiphilic derivative. *Dalton Trans.* **2019**, *48*, 696–710; (b) Phukan, B.; Mukherjee, C.; Goswami, U.; Sarmah, A.; Mukherjee, S.; Sahoo, S. K.; Moi, S. C. A New Bis(aquated) High Relaxivity Mn(II) Complex as an Alternative to Gd(III)-Based MRI Contrast Agent. *Inorg. Chem.* **2018**, *57*, 2631–2638; (c) Khannam, M.; Weyhermüller, T.; Goswami, U.; Mukherjee, C. A Highly Stable L-Alanine-Based Mono(aquated) Mn(II) Complex as a T_1-Weighted MRI Contrast Agent. *Dalton Trans.* **2017**, *46*, 10426–10432.

(6) Inoue, T.; Majid, T.; Pautler, R. G. Manganese Enhanced MRI (MEMRI): Neurophysiological Applications. *Rev. Neurosci.* **2011**, *22*, 675–694.

(7) Rivera-Mancía, S.; Ríos, C.; Montes, S. Manganese accumulation in the CNS and associated pathologies. *Biometals* **2011**, *24*, 811 – 825.

(8) Ndiaye, D.; Sy, M.; Pallier, A.; Même, S.; de Silva, I.; Lacerda, S.; Nonat, A. M.; Charbonnière, L. J.; Tóth, É. Unprecedented Kinetic Inertness for a Mn^{2+}-Bispidine Chelate: A Novel Structural Entry for Mn^{2+}-Based Imaging Agents. *Angew. Chem., Int. Ed.* **2020**, *59*, 11958–11963.

(9) Kálmán, F. K.; Tircsó, G. Kinetic Inertness of the Mn^{2+} Complexes Formed with AAZTA and Some Open-Chain EDTA Derivatives. *Inorg. Chem.* **2012**, *51*, 10065–10067.

(10) Gale, E. M.; Atanasova, I. P.; Blasi, F.; Ay, I.; Caravan, P. A Manganese Alternative to Gadolinium for MRI Contrast. *J. Am. Chem. Soc.* **2015**, *137*, 15548–15557.

(11) Pota, K.; Garda, Z.; Kálmán, F. K.; Luis Barriada, J. L.; Esteban-Gómez, D.; Platas-Iglesias, C.; Tóth, I.; Brücher, E. Tircsó, G. Taking the Next Step Toward Inert Mn^{2+} Complexes of Open-Chain Ligands: The Case of the Rigid PhDTA Ligand. *New J. Chem.* **2018**, *42*, 8001—8011.

(12) Erstad, D. J.; Ramsay, I. A.; Jordan, V. C.; Sojoodi, M.; Fuchs, B. C.; Tanabe, K. K.; Caravan, P.; Gale, E. M. Tumor Contrast Enhancement and Whole-Body Elimination of the Manganese-Based Magnetic Resonance Imaging Contrast Agent Mn-PyC3A. *Invest. Radiol.* **2019**, *54*, 697–703.

(13) Vanasschen, C.; Molnár, E.; Tircsó, G.; Kálmán, F. K.; Tóth, É.; Brandt, M.; Coenen, H. H.; Neumaier. B. Novel CDTA-based, Bifunctional Chelators for Stable and Inert Mn^{II} Complexation: Synthesis and Physicochemical Characterization. *Inorg. Chem.* **2017**, *56*, 7746–7760.

(14) Wang, J.; Wang, H.; Ramsay, I. A.; Erstad, D. J.; Fuchs, B. C.; Tanabe, K. K.; Caravan, P.; Gale, E. M. Manganese-Based Contrast Agents for Magnetic Resonance Imaging of Liver Tumors: Structure–Activity Relationships and Lead Candidate Evaluation. *J. Med. Chem.* **2018**, *61*, 8811–8824.

(15) (a) Baranyai, Z.; Pálinkás, Z.; Uggeri, F.; Maiocchi, A.; Aime, S.; Brücher, E. Dissociation Kinetics of Open-Chain and Macrocyclic Gadolinium(III)-Aminopolycarboxylate Complexes Related to Magnetic Resonance Imaging: Catalytic Effect of Endogenous Ligands. *Chem. Eur. J.* **2012**, *18*, 16426–16435; (b) Baranyai, Z.; Brücher, E.; Uggeri, F.; Maiocchi, A.; Tóth, I.; Andrási, M.; Gáspár, A.; Zékány, L.; Aime, S.. The Role of Equilibrium and Kinetic Properties in the Dissociation of Gd[DTPA-bis(methylamide)] (Omniscan) at near to Physiological Conditions. *Chem. Eur. J.* **2015**, *21*, 4789 – 4799.

(16) Garda, Z.; Molnár, E.; Kálmán, F. K.; Botár, R.; Nagy, V.; Baranyai, Z.; Brücher, E.; Kovács, Z.; Tóth, I.; Tircsó, G. Effect of the Nature of Donor Atoms on the Thermodynamic, Kinetic and Relaxation Properties of Mn(II) Complexes Formed With Some Trisubstituted 12-Membered Macrocyclic Ligands. *Front. Chem.* **2018**, *6*, 232.

(17) Drahos, B.; Kotek, J.; Hermann, P.; Lukes, I.; Tóth, É. Mn^{2+} Complexes with Pyridine-Containing 15-Membered Macrocycles: Thermodynamic, Kinetic, Crystallographic, and ^{1}H/^{17}O Relaxation Studies. *Inorg. Chem.* **2010**, *49*, 3224–3238.

(18) Garda, Z.; Forgács, A.; Do, Q. N.; Kálmán, F. K.; Timári, S.; Baranyai, Z.; Tei, L.; Tóth, I.; Kovács, Z.; Tircsó, G. Physicochemical Properties of Mn^{II} Complexes Formed with *cis*- and

trans-DO2A: Thermodynamic, Electrochemical and Kinetic studies. *J. Inorg. Biochem.* **2016**, *163*, 206–213.

(19) Forgács, A.; Tei, L.; Baranyai, Z.; Tóth, I.; Zékány, L.; Botta, M. A Bisamide Derivative of [Mn(1,4-DO2A)] – Solution Thermodynamic, Kinetic, and NMR Relaxometric Studies. *Eur. J. Inorg. Chem.* **2016**, 1165–1174.

(20) Forgács, A.; Tei, L.; Baranyai, Z.; Esteban-Gómez, D.; Platas-Iglesias, C.; Botta, M. Optimising the relaxivities of Mn^{2+} complexes by targeting human serum albumin (HSA). *Dalton Trans.* **2017**, *46*, 8494–8504.

(21) Botár, R.; Molnár, E.; Trencsényi, G.; Kiss, J.; Kálmán, F. K.; Tircsó, G. Stable and Inert Mn(II)-Based and pH-Responsive Contrast Agents. *J. Am. Chem. Soc.* **2020**, *142*, 1662–1666.

(22) Kálmán, F. K.; Nagy, V.; Váradi, B.; Garda, Z.; Molnár, E.; Trencsényi, G.; Kiss, J.; Même, S.; Même, W.; Tóth, E.; Tircsó, G. Mn(II)-Based MRI Contrast Agent Candidate for Vascular Imaging. *J. Med. Chem.* **2020**, *63*, 6057–6065.

(23) Kim, W. D.; Hrncir, D. C.; Kiefer, G. E.; Sherry, A. D. Synthesis, Crystal Structure, and Potentiometry of Pyridine-Containing Tetraaza Macrocyclic Ligands with Acetate Pendant Arms. *Inorg. Chem.* **1995**, *34*, 2225-2232.

(24) Le Fur, M.; Beyler, M.; Molnár, E.; Fougère, O.; Esteban-Gómez, D.; Tircsó, G.; Platas-Iglesias, C.; Lepareur, N.; Rousseaux, O.; Tripier, R. The Role of the Capping Bond Effect on Pyclen $^{nat}Y^{3+}/^{90}Y^{3+}$ Chelates: Full Control of the Regiospecific N-functionalization Makes the Difference. *Chem. Commun.* **2017**, *53*, 9534—9537.

(25) Kunz, H.; Unverzagt, C. The Allyloxycarbonyl (Aloc) Moiety—Conversion of an Unsuitable into a Valuable Amino Protecting Group for Peptide Synthesis. *Angew. Chem. Int. Ed. Engl.* **1984**, *23*, 436-437.

(26) (a) Dessolin, M.; Guillerez, M.-G.; Thieriet, N.; Guibé, F.; Loffet, A. New Allyl Group Acceptors for Palladium Catalyzed Removal of Allylic Protections and Transacylation of Allyl Carbamates. *Tetrahedron Lett.* **1995**, *36*, 5741-5744; (b) Thieriet, N.; Gomez-Martinez, P.; Guibé, F. Tandem deprotection-coupling of N^{α}-Alloc-amino acids by use of ternary systems Pd cat./PhSiH3/carboxy-activated amino acid. *Tetrahedron Lett.* **1999**, *40*, 2505-2508.

(27) Aime, S.; Botta, M.; Geninatti Crich, S.; Giovenzana, G. B.; Jommi, G.; Pagliarin, R.; Sisti, M. Synthesis and NMR Studies of Three Pyridine-Containing Triaza Macrocyclic Triacetate Ligands and Their Complexes with Lanthanide Ions. *Inorg. Chem.* **1997**, *36*, 2992–3000.

(28) Drahos, B.; Kotek, J.; Císarová, I.; Hermann, P.; Helm, L.; Lukeš, I.; Tóth, É. Mn^{2+} Complexes with 12-Membered Pyridine Based Macrocycles Bearing Carboxylate or Phosphonate Pendant Arm: Crystallographic, Thermodynamic, Kinetic, Redox, and $^{1}H/^{17}O$ Relaxation Studies. *Inorg. Chem.* **2011**, *50*, 12785–12801.

(29) Tircsó, G.; Kovács, Z.; Sherry, A. D. Equilibrium and Formation/Dissociation Kinetics of Some Ln^{III}PCTA Complexes. *Inorg. Chem.* **2006**, *45*, 9269-9280.

(30) Delgado, R.; Quintino, S.; Teixeira, M.; Zhang, A. Metal Complexes of a 12-Membered Tetraaza Macrocycle Containing Pyridine and N-Carboxymethyl Groups. *J. Chem. Soc., Dalton Trans.* **1996**, 55–63.

(31) Takacs, A.; Napolitano, R.; Purgel, M.; Benyei, A. C.; Zekany, L.; Brucher, E.; Tóth, I.; Baranyai, Z.; Aime, S. Solution Structures, Stabilities, Kinetics, and Dynamics of DO3A and DO3A-Sulphonamide Complexes. *Inorg. Chem.* **2014**, *53*, 2858–2872.

(32) Gündüz, S.; Vibhute, S.; Botár, R.; Kálmán, F. K.; Tóth, I.; Tircsó, G.; Regueiro-Figueroa, M.; Esteban-Gómez, D.; Platas-Iglesias, C.; Angelovski, G. Coordination Properties of GdDO3A-Based Model Compounds of Bioresponsive MRI Contrast Agents. *Inorg. Chem.* **2018**, *57*, 5973–5986.

(33) Bianchi, A.; Calabi, L.; Giorgi, C.; Losi, P.; Mariani, P.; Palano, D.; Paoli, P.; Rossi, P.; Valtancoli, B. Thermodynamic and structural aspects of manganese(II) complexes with polyamino-polycarboxylic ligands based upon 1,4,7,10-tetraazacyclododecane (cyclen). Crystal structure of dimeric $[MnL]_2{\cdot}2CH_3OH$ containing the new ligand 1,4,7,10-tetraazacyclododecane-1,4-diacetate. *J. Chem. Soc., Dalton Trans.* **2001**, 917–922.

(34) Esteban-Gómez, D.; Cassino, C.; Botta, M.; Platas-Iglesias, C. ^{17}O and ^{1}H Relaxometric and DFT Study of Hyperfine Coupling Constants in $[Mn(H_2O)_6]^{2+}$. *RSC Adv.* **2014**, *4*, 7094–7103.

(35) Patinec, V.; Rolla, G. A.; Botta, M.; Tripier, R.; Esteban-Gómez, D.; Platas-Iglesias, C. Hyperfine Coupling Constants on Inner-Sphere Water Molecules of a Triazacyclononane-based Mn(II) Complex and Related Systems Relevant as MRI Contrast Agents. *Inorg. Chem.* **2013**, *52*, 11173–11184.

(36) Wen, J.; Geng, Z.; Yin, Y.; Wang, Z. A Mononuclear Mn^{2+} Complex Based on a Novel tris-(ethyl acetate) Pendant-Armed Tetraazamacrocycle: Effect of Pyridine on Self-Assembly and Weak Interactions. *Inorg. Chem. Commun.* **2012**, *21*, 16-20.

(37) (a) Le Fur, M.; Molnár, E.; Beyler, M.; Fougere, O.; Esteban-Gómez, D.; Rousseaux, O.; Tripier, R.; Tircsó, G.; Platas-Iglesias, C. Expanding the Family of Pyclen-Based Ligands Bearing Pendant Picolinate Arms for Lanthanide Complexation. *Inorg. Chem.* **2018**, *57*, 6932-6945; (b) Le Fur, M.; Molnár, E.; Beyler, Kálmán, F. K.; Fougère, O.; Esteban-Gómez, D.; Rousseaux, O.; Tripier, R.; Tircsó, G.; Platas-Iglesias, C. A Coordination Chemistry Approach to Fine-Tune the Physicochemical Parameters of Lanthanide Complexes Relevant to Medical Applications. *Chem. Eur. J.* **2018**, *24*, 3127-3131.

(38) Bader, R. F. W.; Carroll, M. T.; Cheeseman, J. R.; Chang, C. Properties of Atoms in Molecules: Atomic Volumes. *J. Am. Chem. Soc.* **1987**, *109*, 7968-7979.

(39) (a) Fanali, G.; Cao, Y.; Ascenzi, P.; Fasano, M. Mn(II) Binding to Human Serum Albumin: A ^{1}H-NMR Relaxometric Study. *J. Inorg. Biochem.* **2012**, *117*, 198-203; (b) Aime, S.; Canton, S.; Crich, S. G.; Terreno, E. ^{1}H and ^{17}O Relaxometric Investigations of the Binding of Mn(II) ion to Human Serum Albumin. *Magn. Reson. Chem.* **2002**, *40*, 41-48.

(40) Caravan, P.; Farrar, C. T.; Frullano, L.; Uppal, R. Influence of Molecular Parameters and Increasing Magnetic Field Strength on Relaxivity of Gadolinium- and Manganese-Based T1 contrast agents. *Contrast Media Mol. Imaging* **2009**, *4*, 89-100.

(41) Maigut, J.; Meier, R.; Zahl, A.; van Eldik, R. Effect of Chelate Dynamics on Water Exchange Reactions of Paramagnetic Aminopolycarboxylate Complexes. *Inorg. Chem.* **2008**, *47*, 5702-5719.

(42) Harley, S. J.; Ohlin, C. A.; Casey, W. H. Geochemical Kinetics via the Swift–Connick Equations and Solution NMR. *Geochim. Cosmochim. Acta* **2011**, *75*, 3711–3725.

(43) Gale, E. M.; Zhu, J.; Caravan, P. Direct Measurement of the Mn(II) Hydration State in Metal Complexes and Metalloproteins through ^{17}O NMR Line Widths. *J. Am. Chem. Soc.* **2013**, *135*, *49*, 18600-18608.

(44) Loving, G. S.; Mukherjee, S.; Caravan, P.; Redox-Activated Manganese-Based MR Contrast Agent. *J. Am. Chem. Soc.* **2013**, *135*, 4620–4623.

(45) (a) Carli, S.; Benazzi, S.; Casarin, L.; Bernardi, T.; Bertolasi, V.; Argazzi, R.; Caramoria, S.; Bignozzi, C. A. On the stability of manganese tris(β-diketonate) complexes as redox mediators in DSSCs. *Phys. Chem. Chem. Phys.* **2016,** *18,* 5949-5956; (b) Freitag, R.; Conradie, J. Electrochemical and Computational Chemistry Study of Mn(β-diketonato)$_3$ Complexes. *Electrochim. Acta* **2015**, *158*, 418-426.

(46) Ukeda, H.; Kawana, D.; Maeda, S.; Sawamura, M. Spectrophotometric Assay for Superoxide Dismutase Based on the Reduction of Highly Water-Solube Tetrazolium Salts by Xanthine-Xanthine Oxidase. *Biosci. Biotechnol. Biochem.* **1999**, *63*, 485-488.

(47) Fisher, A. E. O.; Naughton, D. P. Metal Ion Chelating Peptides with Superoxide Dismutase Activity. *Biomed. Pharmacother.* **2005**, *59*, 158-162.

(48) Deroche, A.; Morgenstern-Badarau, I.; Cesario, M.; Guilhem, J.; Keita, B.; Nadjo, L.; Houée-Levin, C. A Seven-Coordinate Manganese(II) Complex Formed with a Single Tripodal Heptadentate Ligand as a New Superoxide Scavenger. *J. Am. Chem. Soc.* **1996**, *118*, 4567-4573.

(49) (a) Bonetta, R. Potential Therapeutic Applications of MnSODs and SOD-Mimetics. *Chem. Eur. J.* **2018**, *24*, 5032-5041; (b) Aston, K.; Rath, N.; Naik, A.; Slomczynska, U.; Schall, O. F.; Riley, D. P. Computer-Aided Design (CAD) of Mn(II) Complexes: Superoxide Dismutase Mimetics with Catalytic Activity Exceeding the Native Enzyme. *Inorg. Chem.* **2001**, *40*, 1779-1789.

(50) (a) Bao, J.; Zhang, Z.; Tang, R.; Han, H.; Yang, Z. Synthesis and fluorescence properties of Tb(III) complex with a novelaromatic carboxylic acid (L) as well as spectroscopic studies on the interaction between Tb(III) complex and bovine serum albumin. *J. Lumin.* **2013**, *136*, 68–74; (b) Su, H.; Wu, C.; Zhu, J.; Miao, T.; Wang, D.; Xia, C.; Zhao, X.; Gong, Q.; Song, B.; Ai, H. Rigid Mn(II) Chelate as Efficient MRI Contrast Agent for Vascular Imaging. *Dalton Trans.* **2012**, *41*, 14480-14483.

(51) Irving, H. M.; Miles, M. G.; Pettit, L. A Study of Some Problems in Determining the Stoichiometric Proton Dissociation Constants of Complexes by Potentiometric Titrations Using a Glass Electrode. *Anal. Chim. Acta* **1967**, *38*, 475–488.

(52) Zekany L., Nagypal I. PSEQUAD, in Computational Methods for the Determination of Formation Constants. Modern Inorganic Chemistry. Leggett D. J. (Ed), Springer, Boston, 1985.

(53) Raiford, D. S.; Fisk, C. L.; Becker, E. D. Calibration of Methanol and Ethylene Glycol Nuclear Magnetic Resonance Thermometers. *Anal. Chem.* **1979**, *51*, 2050–2051.

(54) Meiboom, S.; Gill, D. Modified Spin-Echo Method for Measuring Nuclear Relaxation Times. *Rev. Sci. Instrum. 1958*, *29*, 688–691.

(55) Hugi, A. D.; Helm, L.; Merbach, A. E. Water Exchange on Hexaaquavanadium(III): a Variable-Temperature and Variable-Pressure ^{17}O-NMR Study at 1.4 and 4.7 Tesla. *Helv. Chim. Acta* **1985**, *68*, 508–521.

(56) (a) Swift, T. J.; Connick, R. E. NMR-Relaxation Mechanisms of O^{17} in Aqueous Solutions of Paramagnetic Cations and the Lifetime of Water Molecules in the First Coordination Sphere. *J. Chem. Phys.* **1962**, *37*, 307–320. (b) Swift, T. J.; Connick, R. E. NMR-Relaxation Mechanisms of ^{17}O in Aqueous Solutions of Paramagnetic Cations and the Lifetime of Water Molecules in the First Coordination Sphere. *J. Chem. Phys.* **1964**, *41*, 2553.

(57) (a) Yerly, F. VISUALISEUR 2.3.5; Lausanne, Switzerland, 1999; (b) Yerly, F. OPTIMISEUR 2.3.5; Lausanne, Switzerland, 1999.

(58) Gaussian 16, Revision C.01, Frisch, M. J.; Trucks, G. W.; Schlegel, H. B.; Scuseria, G. E.; Robb, M. A.; Cheeseman, J. R.; Scalmani, G.; Barone, V.; Petersson, G. A.; Nakatsuji, H.; Li, X.; Caricato, M.; Marenich, A. V.; Bloino, J.; Janesko, B. G.; Gomperts, R.; Mennucci, B.; Hratchian, H. P.; Ortiz, J. V.; Izmaylov, A. F.; Sonnenberg, J. L.; Williams-Young, D.; Ding, F.; Lipparini, F.; Egidi, F.; Goings, J.; Peng, B.; Petrone, A.; Henderson, T.; Ranasinghe, D.; Zakrzewski, V. G.; Gao, J.; Rega, N.; Zheng, G.; Liang, W.; Hada, M.; Ehara, M.; Toyota, K.; Fukuda, R.; Hasegawa, J.; Ishida, M.; Nakajima, T.; Honda, Y.; Kitao, O.; Nakai, H.; Vreven, T.; Throssell, K.; Montgomery, J. A., Jr.; Peralta, J. E.; Ogliaro, F.; Bearpark, M. J.; Heyd, J. J.; Brothers, E. N.; Kudin, K. N.; Staroverov, V. N.; Keith, T. A.; Kobayashi, R.; Normand, J.; Raghavachari, K.; Rendell, A. P.; Burant, J. C.; Iyengar, S. S.; Tomasi, J.; Cossi, M.; Millam, J. M.; Klene, M.; Adamo, C.; Cammi, R.; Ochterski, J. W.; Martin, R. L.; Morokuma, K.; Farkas, O.; Foresman, J. B.; Fox, D. J. Gaussian, Inc., Wallingford CT, 2016.

(59) Peverati, R.; Truhlar, D. G. Improving the Accuracy of Hybrid Meta-GGA Density Functionals by Range Separation. *J. Phys. Chem. Lett.* **2011**, *2*, 2810-2817.

(60) Weigend, F.; Ahlrichs, R. Balanced basis sets of split valence, triple zeta valence and quadruple zeta valence quality for H to Rn: Design and assessment of accuracy. *Phys. Chem. Chem. Phys.* **2005**, *7*, 3297-305.

(61) Tomasi, J.; Mennucci, B.; Cammi, R. Quantum Mechanical Continuum Solvation Models. *Chem. Rev.* **2005**, *105*, 2999-3093.

(62) (a) Goldstein, S.; Michel, C.; Bors, W.; Saran, M.; Czapski, G. A critical reevaluation of some assay methods for superoxide dismutase activity. *Free Radic. Biol. Med.* **1988**, *4*, 295-303; (b) Lihi, N.; Kelemen, D.; May, N. V.; Fábián, I. The Role of the Cysteine Fragments of the Nickel Binding Loop in the Activity of the Ni(II)-Containing SOD Enzyme. *Inorg. Chem.* **2020**, *59*, 4772-4780.

TOC Graphic:

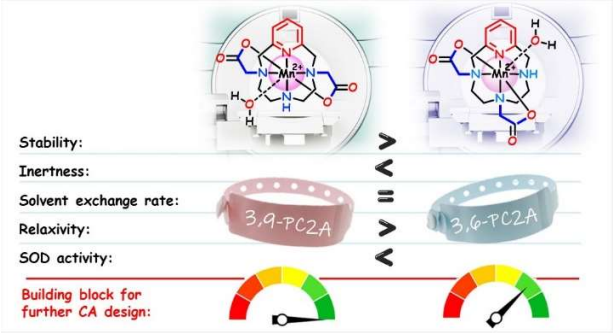

TOC synopsis: Two regioisomeric Mn(II) complexes show promise as building blocks for the preparation of MRI contrast agents.